Biophysical Journal Volume 108 June 2015 2912–2924

Article

Spatial Control of Biochemical Modification Cascades and Pathways

Aiman Alam-Nazki[1] and J. Krishnan[1,2,*]

[1]Department of Chemical Engineering, Centre for Process Systems Engineering and [2]Institute for Systems and Synthetic Biology, Imperial College London, South Kensington Campus, London, United Kingdom

ABSTRACT Information transmission in cells occurs through complex networks of proteins and genes and is relayed through cascades of biochemical modifications, which are typically studied through ordinary differential equations. However, it is becoming increasingly clear that spatial factors can strongly influence chemical information transmission in cells. In this article, we systematically disentangle the effects of space in signaling cascades. This is done by examining the effects of localization/compartmentalization and diffusion of enzymes and substrates in multiple variants of chemical modification cascades. This includes situations where the modified form of species at one stage 1) acts as an enzyme for the next stage; 2) acts as a substrate for the next stage; and 3) is involved in phosphotransfer. Our analysis reveals the multiple effects of space in signal transduction cascades. Although in some cases space plays a modulatory effect (itself of interest), in other cases, spatial regulation and control can profoundly affect the nature of information processing as a result of the subtle interplay between the patterns of localization of species, diffusion, and the nature of the modification cascades. Our results provide a platform for disentangling the role of space and spatial control in multiple cellular contexts and a basis for engineering spatial control in signaling cascades through localization/compartmentalization.

INTRODUCTION

Cells respond to their environment and regulate their internal functioning through complex and sophisticated networks of proteins and genes. Chemical information is transmitted in these networks via various sequences of chemical modifications. The nature of chemical information transmission in signaling cascades is the focus of a large body of work, which has revealed the effects of modifications, the enzymatic regimes, and the effects of enzyme and substrate sequestration.

However, sequences of chemical modifications often involve relevant species moving to different locations where other species may be localized (1). Thus, although modeling and understanding information transmission in signaling cascades through ordinary differential equations provides many useful insights, it completely ignores the spatial dimension of signal transduction. In most studies, spatial aspects are ignored, even if acknowledged, either because they are assumed a priori to be of secondary importance or because the available data are not spatially resolved. At the outset, an implicit assumption often made is that spatial effects can be easily subsumed within a kinetic description through the alteration of relevant kinetic constants, or that it plays a minor role in signal transduction. However, it is not at all clear whether that is indeed the case, or whether spatial factors may introduce important changes in information processing.

We examine the effects of space and localization in different signal transduction cascades. Spatial control through localization and compartmentalization is a recurrent theme in cell biology, observed in many signaling pathways; in addition, localization/compartmentalization through the creation of microcompartments is emerging as an experimental tool in synthetic biology (1–4). We systematically disentangle the interplay of localization, diffusion, and the nature of the modification cascades in a controlled in silico setting. By employing fairly general models and representative scenarios, we aim to tease out the effects of space in signaling cascades. This is contrasted with ordinary differential equation (ODE) models of the cascades, highlighting exactly when and how spatial factors significantly affect and shape signal transduction.

MATERIALS AND METHODS

Our goal is to dissect the effects of space in modification cascades/pathways. One of the most widespread ways in which spatial effects come into play in cells is through localization of entities and modifications. Thus, we largely focus on the effects of space and localization/compartmentalization on various cascades, though we also briefly examine scenarios without localization.

Modification cascades/sequences can arise in different ways in cell signaling. One such scenario is when a modified substrate acts as an enzyme for a subsequent step. Another is when a modified substrate acts as a substrate for a subsequent modification. A third, distinct scenario of modification sequences is through phosphotransfer. These modification sequences are typically studied and understood through ODEs. Stochastic descriptions are invoked to study the effects of small numbers of molecules. Usually, however, the effects of space are ignored. We systematically examine the effects of space and spatial control on these modification sequences by constructing explicit spatial models incorporating the localization and transport of species. The analysis of these spatial models is compared with that of the default ODE models of these processes.

Submitted September 26, 2014, and accepted for publication May 11, 2015.

*Correspondence: j.krishnan@imperial.ac.uk

Editor: Stanislav Shvartsman.

0006-3495/15/06/2912/13 $2.00

http://dx.doi.org/10.1016/j.bpj.2015.05.012

Model setting

We employ multiple models, each describing a different modification sequence. A basic component of most of these models is a covalent modification cycle. A spatial model of this basic enzymatic cycle is described in a standard way by incorporating enzyme binding to substrate (reversibly) to give rise to the complex, which gets irreversibly converted to the modified substrate. The conversion of a protein X to/from its modified version, X^*, involving the kinase K and phosphatase P is described by

$$\frac{\partial[X]}{\partial t} = -k_1[X][E] + k_{-1}[XK] + k_4[X^*P] + D_X\frac{\partial^2[X]}{\partial\theta^2}$$

$$\frac{\partial[X^*]}{\partial t} = -k_3[X^*][P] + k_{-3}[X^*P] + k_2[XK] + D_{X^*}\frac{\partial^2[X^*]}{\partial\theta^2}$$

$$\frac{\partial[K]}{\partial t} = -k_1[X][K] + k_{-1}[XK] + k_2[XK] + D_K\frac{\partial^2[K]}{\partial\theta^2}$$

$$\frac{\partial[P]}{\partial t} = -k_3[X^*][P] + k_{-3}[X^*P] + k_4[X^*P] + D_P\frac{\partial^2[P]}{\partial\theta^2}$$

$$\frac{\partial[XK]}{\partial t} = k_1[X][K] - k_{-1}[XK] - k_2[XK] + D_{XK}\frac{\partial^2[XK]}{\partial\theta^2}$$

$$\frac{\partial[X^*P]}{\partial t} = k_3[X^*][P] - k_{-3}[X^*P] - k_4[X^*P] + D_{X^*P}\frac{\partial^2[X^*P]}{\partial\theta^2},$$

where k_1 and k_3 are the rate constants for binding of the enzymes and their substrate, k_{-1} and k_{-3} are the rate constants for the dissociation of the enzyme-substrate complexes, and k_2 and k_4 are the rate constants for product formation. θ is the spatial coordinate and D_j is the diffusion coefficient for species j. This model includes the diffusion of multiple species and is defined over the entire spatial domain (assumed, for simplicity, to be one-dimensional (1-D)). Different patterns of localization are possible in this cycle (e.g., see our previous work (6)). One scenario corresponds to all species nondiffusible and localized in the same subdomain. Another scenario relevant here is where the entire cycle is localized in a subdomain, apart from one species that exits the domain. The species that are localized in a given region are regarded as nondiffusible (variants of the model involving species diffusing but being prevented from exiting the subdomain are also possible, but these distinctions are not needed here). By allowing X^* alone to diffuse, we then obtain a scenario where X^* can exit the subdomain while other species remain localized. We now turn to the kinetic description of cascades, before describing spatial models.

Enzymatic cascade

When the modified substrate X^* at the first stage is an enzyme for a second modification cycle, the second cycle is described in an analogous way, with X^* playing the role of a kinase, mediating the conversion of Y to Y^*, and the reverse conversion mediated by a phosphatase, $P2$. The kinetic equations for all modification cascades are presented in Section 1 of the Supporting Material. Having components of both modification cycles in the same subdomain, with all species nondiffusible (and present uniformly initially in this subdomain), corresponds to having a localized cascade in a single compartment. This corresponds to an ODE description of the cascade. A schematic of enzymatic cascades is shown in Fig. 1 *A*.

Modification sequence with a common substrate

A different modification sequence results when a modified substrate is modified subsequently by other enzymes. The modification status of a substrate is sometimes referred to as a molecular bar code. If all enzymes and substrates are localized in the same subdomain, assuming a specific ordering to the modification, the modification of X to X^* mediated by the

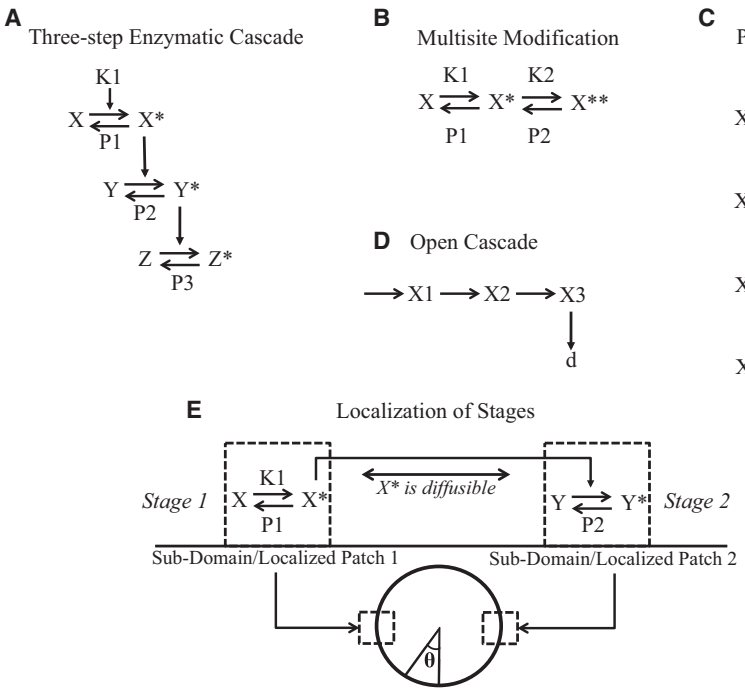

FIGURE 1 Schematic of different kinds of cascades and their localization. (*A*) The three-step enzymatic cascade. The modified substrate in the preceding step acts as the enzyme in the next step. (*B*) Multisite modification. The steps leading to successive modification of a substrate are shown. The relevant enzymes (kinases/phosphatases) for different modifications can be either different (as shown here) or the same. (*C*) Phosphorelay. Shown here is a cascade of four phosphotransfer reactions where the modified substrate transfers its phosphoryl group to the subsequent substrate species. In addition, phosphatases that remove the phosphoryl group may also be present. A special case of this cascade where the phosphatase of the last stage is the kinase of the first stage is also studied. (*D*) Open cascade. A three-stage open cascade is depicted. (*E*) A schematic of the spatial domain and the compartmentalization of a two-step enzymatic cascade in the two subdomains. X^* is the communicating species and diffuses in the spatial domain.

enzyme pair $K1$, $P1$ and the conversion of X^* to X^{**} mediated by the pair $K2$, $P2$ can be described by a basic ODE model. Each elementary modification cycle is described by unpacking the covalent modification cycle in a standard way, as described above. The combination of the description of the two modification cycles provides the ODE model for the sequence of modifications (see Fig. 1 *B*).

Phosphotransfer mechanism

Another basic mechanism of chemical information transmission is via a phosphotransfer. In a two-step phosphorelay, the substrate in the first step, $X1$, is phosphorylated by an enzyme (K1). The phosphorylated form, $X1^*$, transfers its phosphate group to the substrate of the second step, $X2$, producing $X2^*$, resulting in $X1^*$ converting back to $X1$. A phosphatase catalyzes the dephosphorylation of $X2^*$ to $X2$. Different variants of phosphotransfer models exist that vary depending on whether phosphatases exist for individual steps in the cascade (5). We consider a scenario where individual steps have phosphatases, and so $X1^*$ can be dephosphorylated by a phosphatase $P1$ and so on. The ODE model describing the kinetics is presented in the Supporting Material. Other variants of phosphotransfer models were also examined (discussed subsequently). We study the two-step phosphorelay and a four-step phosphorelay (which is observed in nature). Fig. 1 *C* is a schematic of a four-step phosphorelay.

Spatial model

We study spatial models of the above cascades, focusing on the effects of spatially compartmentalizing individual stages. This is done as follows. The first set of modifications and relevant species (one part of the cascade) is localized in one patch/subdomain, and the second set of modifications and relevant species (the other part of the cascade) is localized in a second patch/subdomain (of equal size to the first), diametrically opposite to the first (Fig. 1 *E*). If no species diffuses, the two patches are isolated with no communication and the modification sequence is broken.

We examine the most natural spatial versions of these cascades by allowing the common species of the two different parts of the cascade to diffuse in the spatial domain and reach the second region to effect the next step in the modification sequence. Thus, in the case of the two-step enzymatic modification cascade mentioned above, X^* diffuses out of the first location, reaching the second location, where it catalyzes the modification of the next stage. The species X, $K1$, $XK1$, and X^*P1 all belong in subdomain 1, whereas Y, X^*Y, Y^*P2, and $P2$ all remain in subdomain 2. The species X^* is present in both patches as well as the intervening spatial region. In the case where the modified substrate at the first stage serves as a substrate for the next stage, the modified substrate X^* diffuses in the spatial domain. All other species are present in either the first or the second subdomain. In the two-stage phosphotransfer model, the modified form of the first stage, $X1^*$, diffuses and reaches the second domain and transfers a phosphate group to $X2$, which is localized there. Fig. 1 *E* depicts a two-step cascade with localization, illustrating how different stages are localized in different locations and the connecting agent diffuses through the spatial domain.

We analyze these spatial models (see Section 1 in the Supporting Material), contrasting them with ODE models of these cascades, which correspond to all steps localized in the same location. Note that in the above description individual stages are localized in different locations and we have one species that diffuses to effect a communication between the two locations. Naturally, it is possible to consider more complex scenarios where multiple species may be diffusing, and these can easily be analyzed by simply making other species diffuse in our modeling framework. In this article, we largely restrict ourselves to the scenario described above, as the simplest nontrivial spatial depiction of the cascade. We discuss some aspects of multiple species diffusing in the text and in Section 2.4 of the Supporting material.

The model is cast, for simplicity, in a 1-D spatial domain with periodic boundary conditions (results analogous to those presented here have been obtained for no-flux boundary conditions). Note that the two patches are of equal size and are symmetrically located at diametrically opposite points on the circle (Fig. 1 *E*). Therefore, for the scenarios considered here, the results are exactly equivalent to those with no-flux boundary conditions in a domain half the size. Thus, all essential results are equally valid for both cases and could be relevant to situations involving modification and diffusion of species in the membrane or the cytosol.

Inputs

The modification sequences are initiated by the presence of enzymes for the first stage. These enzymes are assumed to be localized in the first domain and their concentration is varied as part of our analysis.

Parameters

The models of the various cascades involve various kinetic parameters, which can affect enzymatic regimes and information processing. Our approach regarding parametric choices is dictated by the questions of interest. Since the main focus here is on the role of space, and our analysis contrasts the spatial and ODE models, we approach this as follows. We choose a basal set of kinetic parameters (in enzymatic modification/phosphotransfer), which represents enzymatic modification in a generic parameter regime. We separately examine special parameter regimes, such as mass-action or ultrasensitive regimes, to check that similar trends (where applicable) apply here as well. The remaining parameters are the diffusivity of relevant species and the relative sizes of the patches and the overall domain. Again, we choose representative basal values for these parameters. We study the effect of these latter parameters in our analysis. Since we contrast PDE models with ODE models with the same kinetic parameters, we can directly assess the effects of these spatial parameters. In most cases, we perform analytical work to explicitly reveal the influence of parameters and ensure that the essential conclusions are independent of specific kinetic parameters. We emphasize that for the kinds of investigations performed and the nature of conclusions drawn, this approach suffices. If, in some case, a detailed parametric analysis is warranted, it is performed. Parameter values are presented in the Supporting Material.

Numerical method

The PDEs were discretized using finite difference equations and results were checked by doubling the discretization. All simulations were performed in MATLAB using ode15s. In addition, we were able to compare the kinetic parts of our MATLAB models with corresponding models in COPASI (which are automatically generated) for model checking.

RESULTS AND DISCUSSION

Structure of results

Our results for each type of cascade are presented as follows. 1) We examine the behavior of the spatially distributed cascade (in particular, the concentration of the cascade output, which is typically localized) contrasted with ODE models of the cascade that correspond to all stages colocalized; thus, we compare local concentrations. 2) We vary suitable spatial parameters such as the size of the patches or separation between patches, as appropriate. 3) We analyze enzymatic modification cascades, multisite enzymatic and phosphotransfer mechanisms, starting with basic mechanisms and subsequently exploring biologically motivated

variations of each of these. 4) We present computational results backed up by analytical work and tables, presented in the Supporting Material.

The spatial separation of stages of a cascade leads to a dilution effect

We begin by discussing a two-step enzymatic signaling cascade, examining the effect of localization of the two different stages of the cascade at different locations, contrasting this with the situation where all elements are colocalized (Fig. 2 *A*). By contrasting the two situations, we find that the concentration of the output of the cascade (Y^*) is reduced when the modifications occur in different locations. This is understood by noting that when the modification steps are separated, the modified species at the first step, X^*, must diffuse to complete the second modification—as a result, its concentration is spread over the domain, leading to a dilution effect. The concentration of X^* available to the second step is less compared to the scenario where all modifications occur in the same region. Although the concentration of this communicating species increases when the size of the subdomains increases (or the separation decreases), the concentration of the output of the cascade will always be lower for the scenario where the modifications are separated (Fig. 2 *B*). If the separation between the subdomains increases, the output of the cascade will further decrease, as X^* will be spread over a longer domain. The dilution effect occurs because in the course of signaling, the communicating species has to spread in the spatial domain. If there is no de novo production of this species, this spreading results in a decrease of its local concentration. This is demonstrated analytically in Section 2.1 of the Supporting Material.

A second point related to the dilution effect is worth mentioning. We find that when the components of the cascade are separated, the effect of retroactivity is reduced. Specifically, the amount of species X^* sequestered in the downstream complex at steady state is reduced when compared to the case of the completely colocalized cascade. The effect of the second layer of the cascade on the first layer is studied by monitoring the concentration of the complex X^*Y. We find that the retroactivity effect is significantly weakened when compared to the scenario where all species are together (Fig. 2 *C*). This is understood by noting that spatial separation significantly reduces the amount of X^* in the second domain, as discussed, and hence also reduces the amount of X^* sequestered in the second step of the cascade. In Section 2.1 of the Supporting Material, we analytically demonstrate this.

The above discussion reveals the presence of a tradeoff when the two stages of the cascade are separated; at steady state, the output is reduced, and the back-propagating effect of the second stage on the first is also reduced.

The dilution effect can be mitigated under different conditions

The effect of spatial segregation on the steady-state behavior of the cascade discussed above can be reduced under certain conditions. One obvious way to do this is to reduce the spatial separation between the two subdomains. A second way is by designing/operating the cascade in a regime so that the concentration of the communicating species, X^*, is sufficiently low. This can be achieved, for instance, by having a high amount of phosphatase $P1$ in the first domain. In such a situation, the output of the

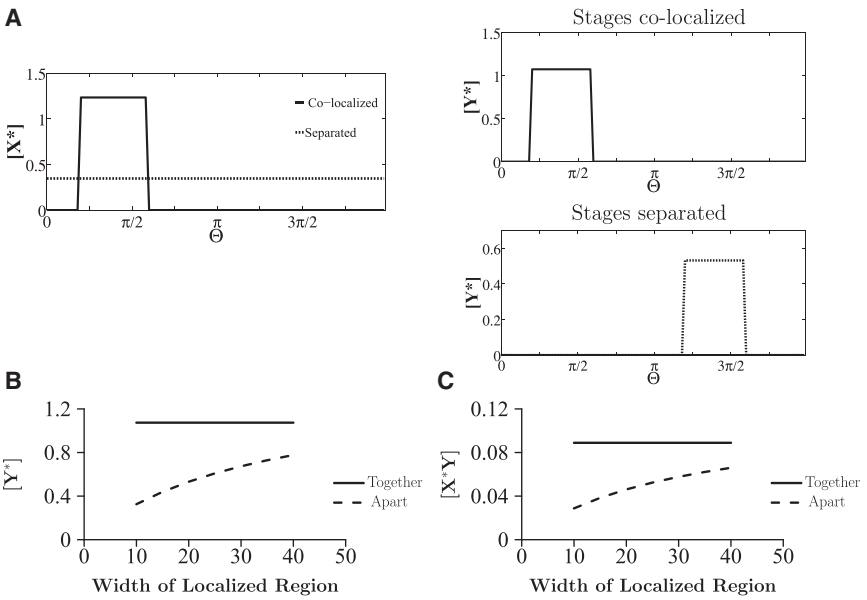

FIGURE 2 Localization in the two-step cascade. Spatial concentration profiles of species in scenarios of complete colocalization and spatial separation of stages are shown. (*A*) In the spatial separation scenario, the concentration of Y^* is reduced as a result of separation of the steps of the cascade, whereas X^* attains a uniform profile. (*B*) $[Y^*]$ is compared between the colocalized (*solid line*) and separated (*dashed line*) scenarios for a range of widths of the localized patches in the domain (as a fraction of total domain size). In the latter case, as the width of the localized region is increased, $[Y^*]$ increases, but it is still less than $[Y^*]$ when all reactions are colocalized. (*C*) The concentration of the complex $[X^*Y]$ in these two cases is shown. A reduction of the steady state $[X^*Y]$ concentration is seen when the stages are separated, implying a reduction in retroactive effects.

spatially separated cascade does not deviate much from that of the colocalized cascade. The reason for this can be explained analytically. 1) At steady state, X^* attains a uniform profile. This is seen by adding all the equations for the species X, X^*, and their complexes. The kinetic terms cancel out, leaving the diffusion term for X^*, and so at steady state, X^* is spatially uniform. 2) If cascade parameters are such that X^* is sufficiently low, this means that the amount of species X that has leaked out of the first compartment is small (relative to the total amount of X species there). The leaking out of X^* results in a modified total concentration of species X in the first domain. 3) The steady states of all X species can be determined from the steady state of the ODEs of the first stage of the cascade, with the modified total X in domain 1, accounting for the leakage. Thus, when the total concentration of species X in domain 1 is modified to a small degree, the steady state of all X species (including X^*) is close to the situation where no X^* exits (the situation of a colocalized cascade). Therefore, the effect on the cascade output, Y^*, induced by spatial separation is negligible, both in absolute and relative terms. This is discussed further analytically in Section 2.1 of the Supporting Material, with Table S1 showing how increasing the phosphatase concentration in domain 1 can result in attenuation of the dilution effect.

Cascades with a Goldbeter-Koshland-type switch

A special case of a cascade is one where an individual stage operates in the ultrasensitive regime. A two-step cascade, where the first step is in the ultrasensitive parameter regime (9) and (for simplicity) the second step operates in the mass-action kinetic regime, with all components colocalized exhibits a switch-like response of the output, Y^*, to the input. In the spatially separated case, this switch-like effect is typically severely attenuated (Fig. S2). This is because the enzymatic cascade at the first layer is now an open system, and the leaking out (due to diffusion) of X^* works against switch-like behavior, in effect making more phosphatase $P1$ available (moving it away from the ultrasensitive regime). It is therefore of interest to see when the switch-like behavior can be maintained in a spatially distributed cascade. One way to achieve this is if the diffusing species is not directly involved in the realizing of the switch. Having an intermediate layer with species I that is modified to I^* catalyzed by X^* (through mass-action kinetics) and I^* diffusing to the new domain (and modifying Y to Y^* there), the switch-like effect can indeed be seen (see Section 2.1 in the Supporting Material). In this case, the input to the diffusing stage of the cascade (the intermediate layer) already contains the switch-like effect: the diffusing stage of the cascade can be treated exactly like the first stage of the cascade we studied previously. However, the amplitude of the switch is reduced due to dilution. This illustrates an aspect relevant to the propagation of switch-like effects in spatially separated enzymatic cascades, where the switch behavior arises primarily from one stage: keeping the factors responsible for a switch localized (negligible leaking out), and propagating the effect via downstream pathways close to mass-action kinetics works to maintain the integrity of the switch.

Three-step cascades with switch-like behavior

We now examine three-step cascades with switch-like behavior, as an extension of the two-step cascades. As a starting point, we use a model of the MAPK cascade developed and analyzed elsewhere (7,8): this describes the three-tier modification cascade of MAPK signaling. We note that some aspects of MAPK signaling, such as the distributive multisite modification at different stages, are not included here. For the purpose of our study, we examine this cascade as an example of one with switch-like behavior. In the model, each modification step is described in the standard way (with explicit description of complexes) and the kinetic parameters employed are from Ventura et al. (8). The ODE model corresponds to the scenario of all species localized in the same domain. Model analysis shows that the cascade exhibits switch-like behavior. In addition, analysis (8) shows that incorporating multisite modification at the second and third stages results in the same qualitative behavior with further sharpening of the switch.

Since the three-tier cascade has three distinct stages, it is clear that there are a number of combinations or spatial designs to spatially partition the cascade. For example, the first stage, associated with modifications of species X, may occur in one location, and those associated with species Y and Z could occur in another location. Another possibility involves stages associated with species X and Y localized in one location and that associated with species Z in another. In the former case, X^* would have to diffuse to the second location to catalyze the modification of Y and in the latter, Y^* would have to diffuse to the second location to complete the modification cascade. Fig. 3 *A* shows four different spatial designs denoted I–IV, involving two different compartments. With an increased possibility of spatial designs, a cell may have more room to exert spatial control over the interactions and achieve a variety of distinct responses.

Input-output responses can be distorted differently with different spatial partitioning of the cascade

The steady-state behavior of the cascade for spatial designs I–IV is examined. This was done for two different relative sizes of the patches (i.e., two different separation distances between them). When the modifications occur in one place, the input-output relationship at steady state is sigmoidal. For the case of a smaller separation (larger relative size of patches), for spatial design II and III, the input-output

A

Spatial Design	Patch Location			Diffusing Entity
	X	Y	Z	
I	1	1	1	None
II	1	1	2	Y*
III	1	2	2	X*
IV	1	2	1	X* and Y*

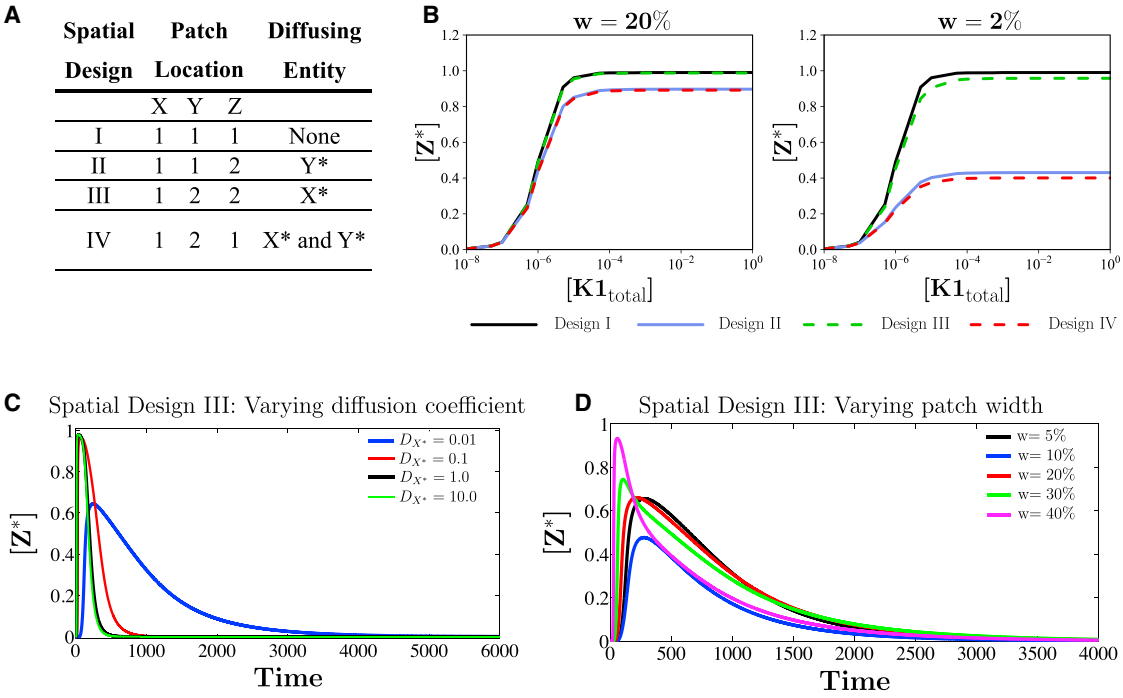

FIGURE 3 Three-step cascade with switch-like behavior: (*A*) Four examples of different spatial compartmentalizations (designs) of the cascade are shown: I) species *X*, *Y*, and *Z* are all together in subdomain 1; II) *X* and *Y* are in subdomain 1 and *Z* is in subdomain 2; III) *X* is in subdomain 1 and *Y* and *Z* are in subdomain 2; IV) *X* and *Z* are in subdomain 1 and Y is in subdomain 2. (*B*) Two sets of steady-state input-output curves are shown, one when the width (*w*) of each localized patch is one-fifth of the domain size (*left*) and the other when the width is one-fiftieth of the domain size (*right*). These plots show that when patch size is smaller (*right*), spatial designs II and IV have a significant effect on the input-output curve. In the larger-patch plot (*left*), the curve for design III is practically indistinguishable from the colocalized case (design I), and the curves for designs II and IV are also practically indistinguishable. For both domain sizes, design III has steady-state input-output curves similar to that of design I. (*C* and *D*) Transient signal input to the cascade, shown for spatial design III. (*C*) The effect of diffusivity of the communicating species (similar trends are seen for other designs) on the transient behavior of the output. (*D*) The duration of the pulse and diffusivity of the communicating species: *X** is fixed. As the patch width increases, a nonmonotonic response is seen: the amplitude of *Z** (shown for the middle of location 2) initially decreases and then increases.

relationship is largely maintained and still appears sigmoidal. The input-output relationship is distorted significantly in the case of larger separation of patches for spatial design II, and the input-output curve becomes much less sigmoidal. However, even with increased separation, for spatial design III, the input-output curve is less distorted and still sigmoidal (Fig. 3 *B*). This shows how different spatial designs can have both subtle and strong effects on cascade behavior (Fig. 3 *B*). It demonstrates that it is possible to design a spatially separated cascade that can largely retain the basic input-output characteristics of the colocalized cascade. The fact that spatial design III leads to a small distortion of the switch can be understood from our analysis of two-step cascades. Here, the kinetic parameters are such that the concentration of the communicating species *X** is typically low relative to total concentrations of species *X* (this is true in the ODEs, too).This is true across the entire range of cascade input where *Z** is sensitive with switch-like behavior. Thus, diffusion of *X** leads to negligible distortion of steady-state input-output characteristics, for the same reason discussed above. For a high enough input, the concentration of *X** can be such that dilution may play a role, but this corresponds to input (and [*X**]) ranges where *Z** is relatively insensitive.

Responses to transient inputs

Our studies of cascades so far have focused on steady states. We now briefly examine pulse inputs of the enzyme K1 to the cascade. Here, we assume, for simplicity, that the input modifies the first stage via mass-action kinetics (this has a very minor effect on the qualitative behavior incidentally), focusing on the concentration of *Z** for different diffusivities of the diffusing species and other spatial parameters.

The effect of diffusivity of communicating species for fixed pulse input

In this section, we examine transient aspects of signaling in spatial design III, subject to a pulse input, focusing on the effect of diffusivity of *X**. As the diffusivity increases, the transient peak concentration of *Z** attained is higher, and the time taken to reach steady state also decreases. Typically, there is appreciable sensitivity of peak concentration

for low diffusivities, whereas less difference is seen between the transient peak concentrations for intermediate and high diffusion coefficient values (Fig. 3 *C*). A similar trend is seen in other designs as well. This indicates how transient behavior of the module output may be shaped by the diffusivity of the communicating species, and that slowly diffusing species can result in strong distortions of transient signaling. This can impose a nontrivial constraint in feasible spatial designs of signaling cascades, for instance in synthetic biology.

The effect of patch size for fixed-pulse duration and diffusivity of communicating species

Note that patch size has no effect when all stages are colocalized together. The transient peak concentration of Z^* typically increases with increasing patch size. Nonmonotonic trends can also be seen in spatial designs III (Fig. 3 *D*) and IV (Fig.S3 *a*). In spatial design III, we find that when the diffusivity of the communicating species is low, as the patch size increases, the transient peak concentration of Z^* first decreases and then increases. Increasing patch size reduces the separation between patches but increases species amounts. The increase in the amount of downstream species can, in a transient regime, result in a reduction of peak Z^* concentration (through sequestration effects).

Switch-like behavior in cascades can arise for particular combinations of parameters, such as the MAPK model parameters. Although numerical results in general can depend on parameters, our analysis shows 1) how switch-like behavior can be significantly distorted, and 2) how it can largely be maintained in a spatial cascade. In the latter case, our analysis of two-step cascades provides relevant insights. Also, similar effects can be expected when the multistep modification at different stages is included (in fact, since the multisite modifications occur in stages 2/3, the minor distortion result in design III is relevant here, too). Our approach provides a framework for elucidating the effects of spatial partitioning in more complex cascades and engineering spatial design of cascades like the MAPK cascade.

Multisite modification

In this module (Fig. 1 *B*), the modified form at the first stage is the substrate for the next step. When the modifications occur in different compartments, the product of the first stage, X^*, has to diffuse to the second location, where the enzymes that catalyze the second modification are present, to complete the sequence of modifications. Having multiple modifications increases the number of spatial designs similar to enzymatic cascades. We focus on the two-site modification module.

The enzymes (kinase, phosphatase) for the first and second modifications are (K1,P1) and (K2,P2), respectively. The ODE model corresponds to all species/modifications in the same compartment. The spatially segregated scenario corresponds to $K1$, $P1$ being present in one location and $K2$, $P2$ in the second location. In the colocalized scenario, the concentration of X^{**} is greater than that of the spatial segregated scenario. Similar to the enzymatic cascade, the dilution effect of the diffusing species, X^*, plays a role. The local concentration of X^*, when it diffuses, is lower everywhere in the spatial domain, and hence, less is available for its conversion to X^{**}. Decreasing the separation between the subdomains, or increasing the size of these subdomains, results in an increase in the steady-state concentration of X^{**}, which is, however, still lower than the colocalized scenario (Fig. 4 *A*). Examining the spatial average concentration of X^* (averaged over the full domain), we find in the spatially segregated scenario that the average concentration of this phosphoform is higher than in the colocalized scenario (Fig. 4 *B*). In fact, the average concentration of X^* increases with spatial separation (these points are discussed in Section 2.2 in the Supporting Material, with analytical work).

We consider a variant of the above case: the first and second modifications are catalyzed by two kinases, $K1$ and $K2$, respectively, and the same phosphatase P1 catalyzes the reverse reactions. When the modifications are in separate locations, the steady-state concentration of X^{**} (and X^*) is zero. This is due to the presence of the enzyme $P1$. $P1$ converts X^{**} to X^* and also converts X^* to X in the second location, leaving only unmodified substrate X in the second location at steady state (Fig. 4 *C*). When the modifications occur in the same compartment, both the modifying enzymes, $K1$ and $K2$, are present together with $P1$ to compensate for the reverse reaction. Thus, nonzero steady states are observed for X^* and X^{**}. Thus, the segregated scenario creates an impediment to obtaining nonzero steady-state response for modified substrates. Alternatively, this segregated scenario may be regarded as creating a new capability for the module, a way to achieve a purely transient/adaptive response (a transient increase in X^{**} in the second location before it falls back down to zero), something which would not occur in the colocalized scenario. If viewed as an impediment, a way in which this can be bypassed is by having both X and X^* diffuse (Fig. 4 *C*). This ensures a continuous cycling of X and X^* between the two patches, resulting in nonzero concentrations of X^{**} at the second location.

We discuss another aspect of spatial control in the case of multisite modification. Our model assumes a specific order for multisite modification, which is implicit in Fig. 1: the modification of the substrate occurs first via $K1$, before $K2$ (and the reverse for the phosphatases). If we examine a random multisite modification mechanism (i.e., either modification can occur first), we see that the spatial separation of kinase-phosphatase pairs we have studied automatically imposes an order for modification, if the unmodified substrate is initially present in one of the compartments. Thus, multisite modification via a random mechanism would still

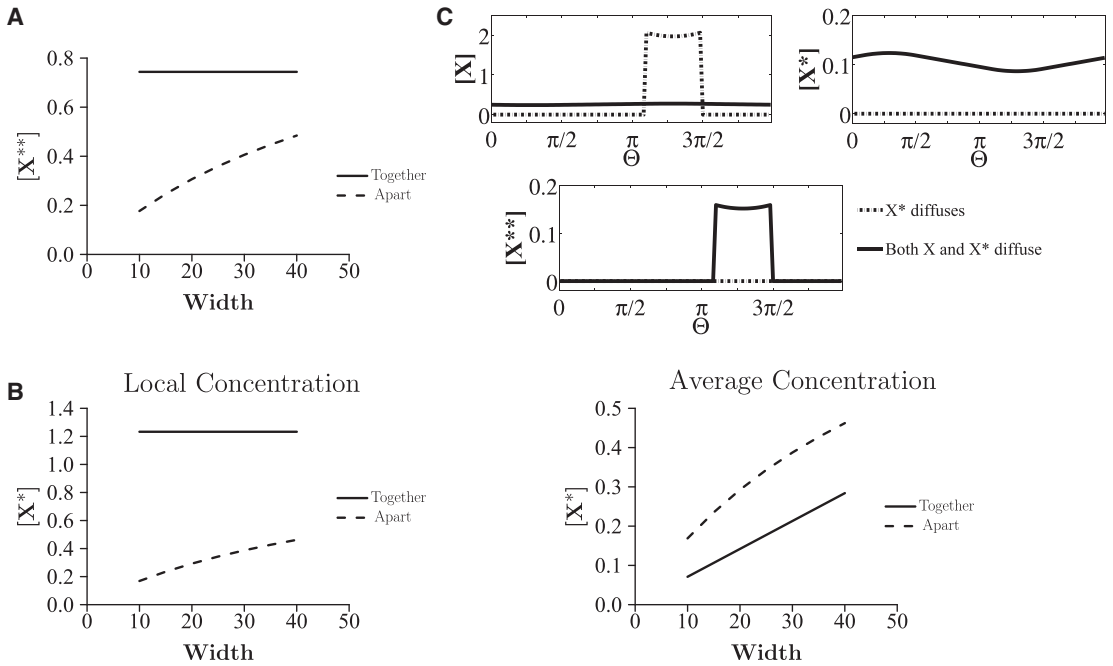

FIGURE 4 Multisite modification. (*A* and *B*) The kinase and phosphatase pairs are different for the two modification steps ($K1$, $P1$ and $K2$, $P2$). (*A*) [X^{**}] is plotted against the width of the localized patch (expressed as a fraction of total domain length): [X^{**}] is always higher when the modifications occur in the same location. The X^{**} concentration increases with the width of the patch. (*B*) The average (over the full domain) and local concentrations of X^* are compared in these cases. The average concentration of X^* is greater when modifications are in different compartments, implying a higher total production of X^* in this case. (*C*) When the kinases for both modification steps are different but the phosphatases are the same (and the modifications take place in separate compartments), at steady state, the concentration of X^{**} will be zero if X^* is the only communicating species (*dash-dotted line*), leaving only X in the second compartment. A way to overcome this locational constraint is by having both X and X^* diffuse in the domain (*solid line*).

proceed in a specific order. If the substrate modified by the second kinase remains localized in the second compartment, this order is maintained and reflected in both transient and steady-state behavior. Spatial control in multisite modification can also occur through localization of kinase(s) and phosphatase(s) at different locations, with substrate cycling between these locations. We briefly discuss this in Section 2.6 in the Supporting Material.

Phosphorelays

In this cascade, an enzyme catalyzes the first phosphorylation step. The product of this step transfers its phosphoryl group to the substrate of the next step, and so on. Phosphatases may be present at every stage. The product of the last step is typically dephosphorylated by a phosphatase. We study two-step relays before turning to four-step relays.

The concentration of the output of the two-step relay, $X2^*$, is compared in the colocalized and spatially segregated scenarios. In the segregated scenario, $X1^*$ (product of the first step) diffuses to a different location and transfers its P group to $X2$ (getting converted back to $X1$). The phosphatase P2 dephosphorylates $X2^*$ back to $X2$; at steady state, both $X1^*$ and $X2^*$ attain a steady-state value of zero. Eventually, only $X1$ and $X2$ are present at steady state at the second location. All the $X1^*$ diffuses out of the first location and gets converted back to $X1$ at the second location, resulting in a zero steady state for $X1^*$ and the relay stalling (Fig. 5 *A*, SM 2.2).

Again, spatial segregation creates a constraint. In contrast to the colocalized scenario, in the segregated case, the concentration of output ($X2^*$) only transiently increases at the second location. This holds true for three- and four-step relays as well (with different spatial designs). Ways to bypass this constraint in two-step relays include 1) removing the phosphatase of the second step; 2), having X1 diffuse (in addition to $X1^*$), which ensures continuous cycling of $X1$ and $X1^*$ between the locations; and 3) having the input signal itself be present everywhere in the spatial domain, or at least at the second location (Fig. 5 *B*); this can reconvert $X1$ to $X1^*$ in the second domain.

An interesting variation of phosphorelays occurs when the input enzyme of the phosphorelay is also the phosphatase of the last step, a situation which can arise through the presence of bifunctional kinases. Such scenarios have been observed in nature (11). We consider spatially distributed phosphorelays, as before, with this enzyme present at both locations (the input and output ends). If we consider a four-step relay and examine the situation where the first three stages occur in one location and the last stage in a different location ($X3^*$ diffuses, effecting the communication), we find that $X4^*$ at steady state is zero (Fig. 5 *C*). In contrast, in a two-step

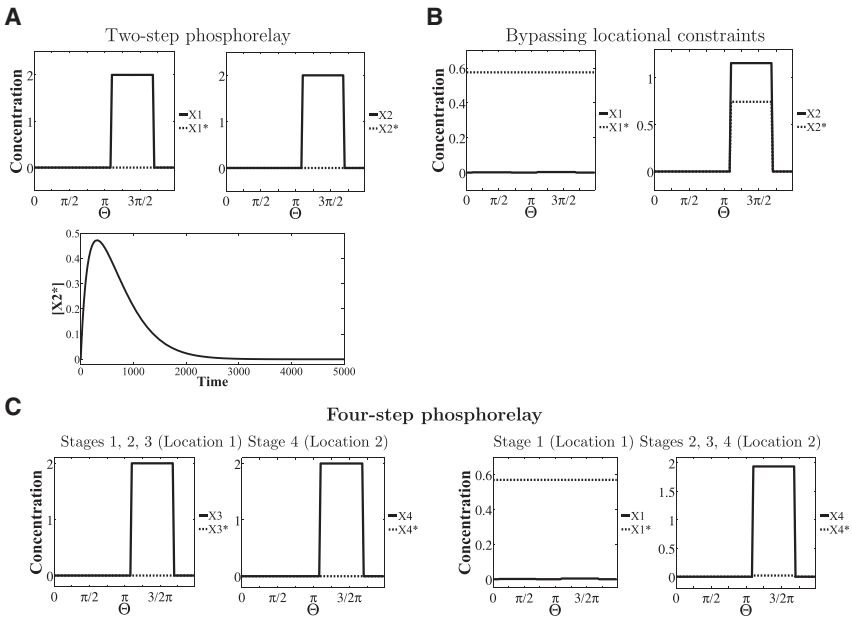

FIGURE 5 Phosphorelay. (*A* and *B*) A two-step phosphorelay (first two stages in Fig. 1 *C*) is considered. (*A*) When the relay steps occur in separate locations (*dashed line*), [*X*2*] only transiently increases (*lower*; [*X*2*] in the middle of the second domain is shown); its steady-state concentration is zero; the steady state of [*X*1*] is also zero. (*B*) A possible way to sustain a nonzero level of *X*2* and bypass this locational constraint is by having a uniform input signal/input at both locations. Shown is the case of a uniform input signal revealing a nonzero output of the cascade. (*C*) A case where the phosphorelay has four steps and the input kinase is a bifunctional enzyme that acts as the kinase (in the first step) and the phosphatase (in the last step) as well is shown. Two spatial designs are shown. In Design 1 (*left*), *X*1, *X*2, and *X*3 are in domain 1 and *X*4 is in domain 2, with *X*3* the communicating/diffusing species. Here, [*X*4*] is zero at steady state. In Design 2 (*right*), *X*1 is in domain 1 and *X*2, *X*3, and *X*4 are in domain 2. *X*1* is the communicating species. Here, the steady state of *X*4* is nonzero (though small). This is because the bifunctional enzyme will ensure that an equilibrium between *X*1* and *X*1 exists at the second location, preventing the relay from stalling. Note that [*X*1] is low but nonzero in both locations in (*B*) and in (*C*, *right*).

cascade with a bifunctional kinase of this kind, the output, *X*2*, can be nonzero, because the bifunctional enzyme at the second location can trigger conversion of *X*1 back to *X*1* at this location. Thus, the presence of a bifunctional enzyme of this kind can allow for nonzero steady states from the output of the phosphorelay. However, in the case of a four-step relay, depending on the spatial partitioning of the cascade, this may or may not be possible. If more than one stage of the relay is localized in the first location, then the presence of a bifunctional enzyme at the second location cannot be used for the purposes of activation (because there is no *X*1 species in this location) and sustaining the phosphorelay. However, this can happen if only the first stage is localized in the first location and all other stages are localized in the second location, with *X*1* diffusing, effecting the communication (see Fig. 5 *C*). This reveals another facet of spatial control of modification cascades.

Open cascades

The examples above involved fixed total amounts of substrates in the spatial domain, whether or not species entered or exited compartments. As a final example, we consider a modification sequence that involves a steady supply of substrate entering and leaving the domain. For concreteness, we examine the irreversible conversion of *X*1 to *X*2 to *X*3 with inflow of *X*1 and outflow of *X*3 (Fig. 1 *D*). Such modification sequences have been studied via ODEs. If a signal causes the conversion of either *X*1 or *X*2, the output of the system *X*3 at steady state is independent of the signal level, and this is thus an example of adaptation: the output recovers to its original prestimulus level, after a step input. This happens irrespective of the position in the cascade where the signal acts.

We now study spatially segregated scenarios. In all cases, *X*1 is present in location 1 and *X*3 in location 2. We first consider the case where the signal modifies *X*2 to *X*3 (in location 2). *X*2, which is produced in the first compartment, diffuses to the other, causing a modification to *X*3 (Fig. S4). An analysis of this scenario shows that in this case, *X*3 does not exhibit (exact) adaptive behavior locally in the second compartment. In fact, *X*3 exhibits spatial variation in the second compartment, whose amplitude is dependent on the signal and diffusivity of *X*2. A simple analysis (Section 2.3 in the Supporting Material) shows that the spatial average of *X*3 is independent of the signal. This shows how localization and spatial separation can change (local) adaptive behavior into nonadaptive behavior, even though adaptation of the average amount of *X*3 occurs. If the diffusion coefficient of *X*2 becomes high, then this effect is reduced. On the other hand, when the signal acts to convert *X*1 to *X*2 (in location 1), we find that the steady-state *X*3 reaches a steady state independent of the signal value, demonstrating that such a spatially distributed open cascade can adapt to signals at certain positions in the cascade. In general, in a cascade of this form, the spatially segregated scenario results in a loss of exact adaptation if the signal acts to convert the diffusible entity.

CONCLUSIONS

Information processing in cells occurs largely through chemical means and involves the movement of molecules

to appropriate locations (1,12–15). Nevertheless, the default method of conceptualizing and understanding information processing in cellular systems is through ODEs, with a few studies focusing on the role of stochasticity. The effect of spatial factors has not been investigated in depth, even though it is clear that spatial control is an important aspect of cellular information processing networks.

One of the most common ways in which spatial control functions in cells is through localization and compartmentalization of components (2,16–18). There are multiple biological examples of this, which echo some of the scenarios we have studied. In enzymatic modification cascades in MAPK signaling and Fox-O signaling, certain entities in the cascade translocate to a new location (e.g., the nucleus) to complete the cascade (17,19,20). In general, the phosphorylation/modification status of a protein is a natural chemical mechanism to control its transport, especially out of/into compartments, and there are multiple examples of this both in single-site and multisite phosphorylation (21–25). The phosphorylated protein may be further modified in the new compartment. Cascades and pathways with phosphorelays are encountered in bacteria, in some cases with spatial control (26). Open cascades have been implicated and studied in the context of homeostatic mechanisms (27–29). We focused on the effect of localization/compartmentalization on modification cascades by creating and analyzing explicit spatial models of these cascades, incorporating localization of species in different locations, providing an appropriate controlled setting. This is relevant both for understanding existing cascades/pathways in cells and imposing spatial control of pathways by synthetic and other means.

Although some studies of compartmentalization/spatial behavior of cascades exist (30–32), our study brings together a global view of spatial control by considering different scenarios, explicit spatial description, and a framework through which we can study the effects of both compartmentalization and diffusion, as well as their interplay (also see our previous article (33)). Although we largely focused on localization, we also studied the effects of diffusion in enzymatic cascades without localization, revealing retroactive effects of species diffusion (see Section 2.5 in the Supporting Material). The global approach undertaken reveals parallels and essential differences between different modification cascades. Through explicit spatial models, we can dissect the effect of many factors, including compartment size and separation, diffusivity of one or more species, etc. Although compartmental ODE models can provide useful insights in some cases, explicit spatial models are necessary for any systematic understanding of spatial regulation and localization, some aspects of which cannot be captured properly in simple compartmental ODE models (e.g., transient effects or effects of intervening medium). This is especially relevant in the cascades/pathways studied, where nonlinearity, conservation of species, and their interplay play vital roles. Although we briefly discuss the effects of multiple species diffusion (see Section 2.4 in the Supporting Material), our framework allows for a systematic exploration to be undertaken in the future. Our models have been developed in 1-D, and as such, they capture the interplay of basic spatial effects that are equally relevant in 2-D and 3-D. Naturally, there are different aspects in 2-D and 3-D that will need additional investigation through dedicated 2-D/3-D models, which can build on the insights obtained here and may be facilitated by software such as Virtual Cell (vcell.org).

Our study of enzymatic cascades reveals firstly that localization of stages at different spatial locations can result in a strongly diminished response. Second, by tuning kinetic parameters/phosphatase concentrations in the cascade, it is possible to buffer against this to a large extent. Third, we find that localization and separation of stages in a cascade can reduce steady state retroactive effects. It is likely that this may be a basic mechanism by which retroactivity is reduced and/or suppressed in multiple cellular contexts. By studying three-step cascades, we find that spatial separation can strongly reduce switch-like behavior in cascades, in agreement with Takahashi et al. (10). We find here that depending on the spatial design of the cascade, it is possible that the switch-like characteristic is largely preserved. These results point to different aspects of the interplay between enzymatic cascades and spatial organization.

Our analysis of multisite-modification mechanisms reveals that through compartmentalization, a random enzymatic modification mechanism (with multiple enzymes) can be converted to an ordered mechanism. In addition, spatially averaging the results across the domain (done when measurements are taken at the cellular level) masks and distorts important aspects of the behavior of these pathways. If different modifications involve a common phosphatase, then the spatially separated modification scheme results in a purely transient increase of the modified phosphoforms, settling at a zero steady state, completely converse to the ODE models. This results from the fact that at the downstream location, the phosphatase is able to reverse phosphorylation for both the full and partial phosphoforms. In such cases, an additional cellular mechanism is then needed to synthesize/transfer relevant substrate to the original location to replenish it. Phosphorelay cascades (in contrast to enzymatic cascades) again reveal similar behavior if different steps of the cascade are separated. Interestingly, a phosphorelay cascade with the phosphatase of the last step acting as a bifunctional kinase (a design observed in nature) can allow the phosphorelay to function (in certain cases) even with compartmentalization, relieving the above constraint.

Space, and in particular spatial localization, is a recurrent theme in cellular systems. Its importance has been acknowledged in the biological literature, and yet the consequences of localization have not been examined systematically

across different kinds of cascades. Spatial localization and control of signaling is relevant from multiple viewpoints: as a basic ingredient in the evolution of information processing networks, as a source of complexity in elucidating information processing and decision making in cells, and as a new mode of control for synthetic biology. We discuss the consequences of our results in relation to these themes.

The evolution of biological networks has resulted in a marked increase in the complexity of signaling pathways as one progresses from bacteria to eukaryotes. This is due to an increased number of components, new modes of interaction, increased feedback regulation, and new entities that are parts of the signaling pathways. Even though localization is present in bacteria as well, it is clear that there are many additional ways of compartmentalization/localization in eukaryotes with the increased number of compartments possible. This indicates that with all the additional complexity of signaling components in eukaryotes, spatial localization may provide important capabilities for realizing different modes of information processing while also bypassing existing constraints. Of course, depending on the context, localization may itself impose important constraints in information processing.

At the outset, it is not easy to guess the rules by which evolution works. The general belief is that evolution works by tinkering with existing networks and circuits, refining, adding and perhaps deleting elements. Naturally, with a substantially increased number of components and possibility of interactions, the complexity of a signal transduction network greatly increases, also increasing the possibility of undesirable interactions. One basic capability provided by localization of components in different places is the insulation of parts of a pathway from the other, minimizing extraneous interactions and unwanted cross talk. Thus, even for a desired mode of information processing (e.g., a switch) the spatially distributed solution may provide a new, more robust alternative. For such a spatially distributed design, our analysis provides insights into how a spatially distributed cascade (with the same kinetic properties) may be organized or optimally partitioned to give rise to a switch. Correspondingly, if the spatially distributed nature of a pathway is given, it may be possible to make local kinetic refinements and arrive at a robust switch-like behavior of the cascade that works around the spatial constraints. In addition, as we have discussed, it is possible to use localization as a mechanism to generate new modes of signal transduction as well, without extraneous kinetic interactions. It is then possible to employ additional refinements to such mechanisms to generate new, more robust circuits exhibiting this behavior.

A default method for studying information processing in signaling pathways is through ODEs. ODEs make an assumption about well-mixed systems with sufficient numbers of molecules so as to justify the kinetic descriptions. Even in some cases where these assumptions may not strictly be met, the ODE description may provide an adequate initial description of the system, essentially because the ODE encodes a form of causal interaction that is the dominant factor in the information processing. The ODEs may be modeled and the results compared with data that implicitly make similar assumptions. Tools of reverse engineering of networks make similar assumptions. Although a widespread, and generally sensible, approach is to develop a model (and employ an appropriate framework) based on the available data, it is also important to examine the actual combination of factors that gives rise to the relevant behavior. As our study indicates, spatial localization results in both modulatory and drastic changes in signal transduction characteristics. Although in some cases a spatial model may be essentially subsumed within a kinetic description, in other cases, as we have seen, this is simply not the case. Modeling such processes with ODEs may then involve invoking additional pathways/feedback effects that may simply be incorrect. Likewise, making measurements using spatial averages (as is done by lysing cells) may simply distort the actual picture.

These aspects come to the fore especially in the presence of strong nonlinearity, which is, of course, a basic and widespread element in signaling pathways. Likewise, other tools for analyzing circuits, including the robustness of circuits, usually employ ODE models. It is very possible that spatial localization and compartmentalization may in fact be a key aspect relevant to the robustness of the circuit. It is also interesting to note that one of the recurrent themes in signal transduction has been the effects of sequestration (34–38) and how this can result in monostable switches (through molecular titration), retroactivity and even bistability (through enzyme sharing for instance). When we examine spatially distributed signaling pathways, we find that some of these effects may in fact be reduced simply due to the spatial compartmentalization and separation, which results in open systems. On the other hand, it may also happen that spatial separation can actually work to accentuate some of this behavior. For instance, spatial separation and the dilution effect discussed above can result in altered availability of enzymes in one compartment, allowing for a regime of bistability, if this is an intrinsic capability of the enzymatic mechanism (as in multisite phosphorylation by a single kinase/phosphatase pair).

Another tool being used to understand different aspects of cellular decision making is information theory (39). Information theory itself relies on some basic abstractions and assumptions, describing the communication process in unidirectional terms, incorporating information encoding, transmission, and decoding. The spatially localized and separate steps we have studied in some respects come close to depicting such a scenario. Our studies demonstrate that specific physiochemical aspects such as the nature of the chemical modification, the spatial location of auxilliary chemical entities, and the size of the domain play a vital

role in how chemical information is actually transmitted and processed.

The spatial regulation of information is also directly relevant to spatial control of pathways through synthetic and other means. In the recent past, experimental approaches in synthetic biology have employed scaffolds to manipulate and shape signal transduction (40). The recent development of microcompartments is another step in this direction (4,41–43). The development of a theoretical framework allows for a systematic exploration of capabilities and constraints associated with the spatial manipulation of information processing, using building blocks available to cells along with additional engineered components. It brings to light hidden tradeoffs involved in this process, and could suggest ways to design synthetic circuits engineered with explicit spatial organization. In combination with new and emerging experimental capabilities, it provides a systematic platform for employing tools that harness or manipulate spatial aspects to shape signal transduction and pathway behavior in general. Finally, this is also relevant in related emerging areas, such as molecular communication and chemical information processing/computing (44,45), each of which deals with the transmission of information through molecular transport and interaction.

SUPPORTING MATERIAL

Supporting Material and seven figures are available at http://www.biophysj.org/biophysj/supplemental/S0006-3495(15)00497-X.

AUTHOR CONTRIBUTIONS

Both authors designed the study, performed the research, and directly contributed to the results presented; J.K. wrote the article with input from A.A-N.

ACKNOWLEDGMENTS

A.A-N. gratefully acknowledges funding through an Engineering and Physical Sciences Research Council DTA fellowship.

REFERENCES

1. Hurtley, S. 2009. Spatial cell biology. Location, location, location. Introduction. *Science.* 326:1205.
2. Shapiro, L., H. H. McAdams, and R. Losick. 2009. Why and how bacteria localize proteins. *Science.* 326:1225–1228.
3. Kam, L. C., K. Shen, and M. L. Dustin. 2013. Micro- and nanoscale engineering of cell signaling. *Annu. Rev. Biomed. Eng.* 15:305–326.
4. Chen, A. H., and P. A. Silver. 2012. Designing biological compartmentalization. *Trends Cell Biol.* 22:662–670.
5. Knudsen, M., E. Feliu, and C. Wiuf. 2012. Exact analysis of intrinsic qualitative features of phosphorelays using mathematical models. *J. Theor. Biol.* 300:7–18.
6. Alam-Nazki, A., and J. Krishnan. 2013. Covalent modification cycles through the spatial prism. *Biophys. J.* 105:1720–1731.
7. Huang, C.-Y., and J. E. Ferrell, Jr. 1996. Ultrasensitivity in the mitogen-activated protein kinase cascade. *Proc. Natl. Acad. Sci. USA.* 93:10078–10083.
8. Ventura, A. C., J. A. Sepulchre, and S. D. Merajver. 2008. A hidden feedback in signaling cascades is revealed. *PLOS Comput. Biol.* 4:e1000041.
9. Goldbeter, A., and D. E. Koshland, Jr. 1981. An amplified sensitivity arising from covalent modification in biological systems. *Proc. Natl. Acad. Sci. USA.* 78:6840–6844.
10. Takahashi, K., S. Tanase-Nicola, and P. R. ten Wolde. 2010. Spatio-temporal correlations can drastically change the response of a MAPK pathway. *Proc. Natl. Acad. Sci. USA.* 107:2473–2478.
11. Chen, Y. E., C. G. Tsokos, …, M. T. Laub. 2009. Dynamics of two Phosphorelays controlling cell cycle progression in *Caulobacter crescentus*. *J. Bacteriol.* 191:7417–7429.
12. Marks, F., U. Klingmuller, and K. Muller-Decker. 2009. Cellular signal processing: an introduction to the molecular mechanisms of signal transduction. Garland Science, New York.
13. Vartak, N., and P. Bastiaens. 2010. Spatial cycles in G-protein crowd control. *EMBO J.* 29:2689–2699.
14. Brown, G. C., and B. N. Kholodenko. 1999. Spatial gradients of cellular phospho-proteins. *FEBS Lett.* 457:452–454.
15. Kholodenko, B. N. 2006. Cell-signalling dynamics in time and space. *Nat. Rev. Mol. Cell Biol.* 7:165–176.
16. Laloux, G., and C. Jacobs-Wagner. 2014. How do bacteria localize proteins to the cell pole? *J. Cell Sci.* 127:11–19.
17. Cyert, M. S. 2001. Regulation of nuclear localization during signaling. *J. Biol. Chem.* 276:20805–20808.
18. Rudner, D. Z., Q. Pan, and R. M. Losick. 2002. Evidence that subcellular localization of a bacterial membrane protein is achieved by diffusion and capture. *Proc. Natl. Acad. Sci. USA.* 99:8701–8706.
19. Kondoh, K., S. Torii, and E. Nishida. 2005. Control of MAP kinase signaling to the nucleus. *Chromosoma.* 114:86–91.
20. Eijkelenboom, A., and B. M. T. Burgering. 2013. FOXOs: signalling integrators for homeostasis maintenance. *Nat. Rev. Mol. Cell Biol.* 14:83–97.
21. Blenis, J., and M. D. Resh. 1993. Subcellular localization specified by protein acylation and phosphorylation. *Curr. Opin. Cell Biol.* 5:984–989.
22. Walsh, C. 2005. Post-translational Modification of Proteins:Expanding Nature's Inventory. Roberts, Greenwood Village, CO.
23. Engel, K., A. Kotlyarov, and M. Gaestel. 1998. Leptomycin B-sensitive nuclear export of MAPKAP kinase 2 is regulated by phosphorylation. *EMBO J.* 17:3363–3371.
24. Goyal, P., D. Pandey, and W. Siess. 2006. Phosphorylation-dependent regulation of unique nuclear and nucleolar localization signals of LIM kinase 2 in endothelial cells. *J. Biol. Chem.* 281:25223–25230.
25. Cohen, P. 2000. The regulation of protein function by multisite phosphorylation—a 25 year update. *Trends Biochem. Sci.* 25:596–601.
26. Thanbichler, M. 2009. Spatial regulation in *Caulobacter crescentus*. *Curr. Opin. Microbiol.* 12:715–721.
27. Csikász-Nagy, A., and O. S. Soyer. 2008. Adaptive dynamics with a single two-state protein. *J. R. Soc. Interface.* 5 (*Suppl 1*):S41–S47.
28. Drengstig, T., I. W. Jolma, …, P. Ruoff. 2012. A basic set of homeostatic controller motifs. *Biophys. J.* 103:2000–2010.
29. Kerkeb, L., I. Mukherjee, …, E. L. Connolly. 2008. Iron-induced turnover of the Arabidopsis IRON-REGULATED TRANSPORTER1 metal transporter requires lysine residues. *Plant Physiol.* 146:1964–1973.
30. Bhalla, U. S. 2011. Trafficking motifs as the basis for two-compartment signaling systems to form multiple stable states. *Biophys. J.* 101:21–32.
31. Berezhkovskii, A. M., M. Coppey, and S. Y. Shvartsman. 2009. Signaling gradients in cascades of two-state reaction-diffusion systems. *Proc. Natl. Acad. Sci. USA.* 106:1087–1092.

32. Harrington, H. A., E. Feliu, …, M. P. H. Stumpf. 2013. Cellular compartments cause multistability and allow cells to process more information. *Biophys. J.* 104:1824–1831.

33. Alam-Nazki, A., and J. Krishnan. 2012. An investigation of spatial signal transduction in cellular networks. *BMC Syst. Biol.* 6:83.

34. Buchler, N. E., and M. Louis. 2008. Molecular titration and ultrasensitivity in regulatory networks. *J. Mol. Biol.* 384:1106–1119.

35. Del Vecchio, D., A. J. Ninfa, and E. D. Sontag. 2008. Modular cell biology: retroactivity and insulation. *Mol. Syst. Biol.* 4:161.

36. Feliu, E., and C. Wiuf. 2012. Enzyme-sharing as a cause of multi-stationarity in signalling systems. *J. R. Soc. Interface.* 9:1224–1232.

37. Blüthgen, N., F. J. Bruggeman, …, B. N. Kholodenko. 2006. Effects of sequestration on signal transduction cascades. *FEBS J.* 273:895–906.

38. Seaton, D. D., and J. Krishnan. 2011. The coupling of pathways and processes through shared components. *BMC Syst. Biol.* 5:103.

39. Shannon, C. E. 1948. A mathematical theory of communication. *Bell Syst. Tech. J.* 27:379–423.

40. Good, M. C., J. G. Zalatan, and W. A. Lim. 2011. Scaffold proteins: hubs for controlling the flow of cellular information. *Science.* 332:680–686.

41. Agapakis, C. M., P. M. Boyle, and P. A. Silver. 2012. Natural strategies for the spatial optimization of metabolism in synthetic biology. *Nat. Chem. Biol.* 8:527–535.

42. Sachdeva, G., A. Garg, …, P. A. Silver. 2014. In vivo co-localization of enzymes on RNA scaffolds increases metabolic production in a geometrically dependent manner. *Nucleic Acids Res.* 42:9493–9503.

43. Peters, R. J. R. W., M. Marguet, …, S. Lecommandoux. 2014. Cascade reactions in multicompartmentalized polymersomes. *Angew. Chem. Int. Ed. Engl.* 53:146–150.

44. Nakano, T., A. W. Eckford, and T. Haraguchi. 2013. Molecular Communication. Cambridge University Press, Cambridge, United Kingdom.

45. Katz, E. 2012. Biomolecular Information Processing: From Logic Systems to Smart Sensors and Actuators. Wiley, Hoboken, NJ.

Spatial control of biochemical modification cascades and pathways: Supplementary material

Aiman Alam-Nazki [1] and J. Krishnan [1,2]

[1] Chemical Engineering and Chemical Technology, Centre for Process Systems Engineering and
[2] Institute for Systems and Synthetic Biology, Imperial College London, South Kensington Campus, London SW7 2AZ, UK.
j.krishnan@imperial.ac.uk. Ph: 44-20-7594-6633; Fax: 44-20-7594-6606.

In this document, we present analysis of a number of aspects of topics discussed in the main text. We present, in turn: (i) The models of the modification cascades (ii) Analysis of different aspects of enzymatic cascades, multisite modifications and phosphotransfer mechanisms (iii) Spatial aspects of open signalling cascades. (iv)Analysis of a single tier of a modification cascade with multiple diffusible entities. (v) Response of a two-tier enzymatic modification cascade to spatial gradients (vi) Multisite modification with separated kinase and phosphatase

1 Models

1.1 Cascade

We present the various models which we will study. The primary focus of the paper was to study the effects of compartmentalization on different kinds of cascades. We present the relevant model equations for these different cascades. At the end of each model, we discuss how different variants of each case we have studied are implemented in the model. Fig. S1 depicts a schematic of some of these modification cascades depicting the reactions in the cascade and the compartment in which they occur. The common species of the two compartments diffuses from one compartment through the intervening space (this is not depicted) and into the second compartment.

We first start with an enzymatic 2-step cascade. We first describe a general spatial model of a 2-step cascade. We then discuss how we adapt this to describe a 2-step cascade with spatial localization, as depicted in Fig. S1.

A general spatial model of a 2-stage enzymatic cascade (in one spatial dimension, with periodic boundary conditions, with the spatial variable being denoted by θ) is described by the following equations:

$$
\begin{aligned}
\frac{\partial[X]}{\partial t} &= -k_1[X][K1] + k_{-1}[XK1] + k_4[X^*P1] + D_X\frac{\partial^2[X]}{\partial\theta^2} \\
\frac{\partial[X^*]}{\partial t} &= -k_3[X^*][P1] + k_{-3}[X^*P1] + k_2[XK1] - k_5[Y][X^*] + k_{-5}[X^*Y] + k_6[X^*Y] + D_{X^*}\frac{\partial^2[X^*]}{\partial\theta^2} \\
\frac{\partial[K1]}{\partial t} &= -k_1[X][K1] + k_{-1}[XK1] + k_2[XK1] + D_{K1}\frac{\partial^2[K1]}{\partial\theta^2} \\
\frac{\partial[P1]}{\partial t} &= -k_3[X^*][P1] + k_{-3}[X^*P1] + k_4[X^*P1] + D_{P1}\frac{\partial^2[P1]}{\partial\theta^2} \\
\frac{\partial[XK1]}{\partial t} &= k_1[X][K1] - k_{-1}[XK1] - k_2[XK1] + D_{XK1}\frac{\partial^2[XK]}{\partial\theta^2} \\
\frac{\partial[X^*P1]}{\partial t} &= k_3[X^*][P1] - k_{-3}[X^*P1] - k_4[X^*P1] + D_{X^*P1}\frac{\partial^2[X^*P1]}{\partial\theta^2} \\
\frac{\partial[Y]}{\partial t} &= -k_5[Y][X^*] + k_{-5}[X^*Y] + k_8[Y^*P2] + D_Y\frac{\partial^2[Y]}{\partial\theta^2} \\
\frac{\partial[Y^*]}{\partial t} &= -k_7[Y^*][P2] + k_{-7}[Y^*P2] + k_6[X^*Y] + D_{Y^*}\frac{\partial^2[Y^*]}{\partial\theta^2} \\
\frac{\partial[P2]}{\partial t} &= -k_7[Y^*][P2] + k_{-7}[Y^*P2] + k_8[Y^*P2] + D_{P2}\frac{\partial^2[P2]}{\partial\theta^2} \\
\frac{\partial[X^*Y]}{\partial t} &= k_5[Y][X^*] - k_{-5}[X^*Y] - k_6[X^*Y] + D_{X^*Y}\frac{\partial^2[X^*Y]}{\partial\theta^2} \\
\frac{\partial[Y^*P2]}{\partial t} &= k_7[Y^*][P2] - k_{-7}[Y^*P2] - k_8[Y^*P2] + D_{Y^*P2}\frac{\partial^2[Y^*P2]}{\partial\theta^2}
\end{aligned}
\tag{1}
$$

The above model is simply a depiction of all the kinetic steps in this cascade, described in a standard way, along with the diffusion of each species. The substrate species are X, X^* (and corresponding complexes XK and X^*P1) in the first level of the cascade and in the second level of the cascade, the substrate species (and relevant complexes) are Y, X^*Y, Y^* and Y^*P2. The enzymes for the first stage of the cascade are K (kinase) and P1 (phosphatase). X^* acts as a kinase for the second level of the cascade and $P2$ is the phosphatase. The model encapsulates a fairly standard and broadly used description of the catalytic conversion of substrate by enzyme, explicitly incorporating enzyme-substrate binding/unbinding and irreversible conversion. This kinetic description of the cascade has been used in multiple studies of signalling cascades.

The rate constants of binding of enzyme to substrate are k_1 (K to X), k_3 (P1 to X^*), k_5 (X^* to Y) and k_7 (P2 to Y^*), while the corresponding unbinding constants are denoted by k_{-1}, k_{-3}, k_{-5} and k_{-7} respectively. The relevant catalytic rate constants for these reactions are denoted by k_2, k_4, k_6 and k_8 respectively. The diffusion coefficients are $D_X, D_{K1}, D_{XK1}, D_{X^*}, D_{P1}, D_{X^*P1}, D_Y, D_{X^*Y}, D_{Y^*}, D_{P2}$ and D_{Y^*P1}, where the subscript denotes the species under consideration.

While this is a general spatial model of a 2 step cascade, we now discuss how we employ this in the context of our results.

Response to a gradient. When we aim to study the response of the model to a spatial input gradient, (see section 2.5 below) we incorporate an explicit description of the input, which is the kinase K. There are different ways in which this can be incorporated. One way is to impose a particular free kinase concentration, described by an equation of the form

$$\frac{\partial [K1]}{\partial t} = -k_1[X][K1] + k_{-1}[XK1] + k_2[XK1] + k_{f1}S(\theta) - k_{b1}[K1] + D_{K1}\frac{\partial^2 [K1]}{\partial \theta^2} \tag{2}$$

This describes a production of K1 by an external signal S and removal of K1 (rate constants k_{f1} and k_{b1}) in addition to the other reactions it is involved in. A similar input has been used in (1).

Localization. The primary focus of the paper is to study the effects of localization (and separation) of different steps of the cascade. Thus, we describe localization in the two step cascade as follows. For simplicity, we will assume that all species are essentially non-diffusible apart from the species conveying the information from one location to the other. Other variants such as those where all localized species also diffuse in the individual compartments (but are confined there) can also be employed but we will not require these additional details for the purposes of our investigations here. We thus have K1, P1 and X in location 1, while Y, Y^* and P2 are in location 2. All relevant enzyme substrate complexes are in the respective locations, and these are assumed non-diffusible. X^* is the diffusible species and thus it is present everywhere in the domain. Therefore in our model we employ suitable initial conditions consistent with this scenario, and make all variables non-diffusible except the communicating variable. This then results in the model of the 2-step cascade with compartmentalization.

We employ the model in a periodic domain with the two locations (of equal size) symmetric and diametrically opposite to one another (see Fig. 1). This also exactly corresponds to no-flux boundary conditions in a domain of half the size.

When we study localization, we thus localize $K1$ in the first location (and the relevant complex is contained here as well). The total concentration of kinase (free + complex) is automatically conserved. The total concentration of $K1$ (free +complex) can be regarded as the input to the cascade. Before the input is applied, there is no modified form X^* present (no K1 present before stimulus).

Three Step Cascade. A three step cascade may be described in an analogous manner. The only difference here is that there is more than one way to spatially partition a three step cascade. For instance,

one possibility is that the first two steps are localized in location 1 and the last step is localized in location 2. Alternatively it is possible that the first step is in location 1 (just like the two step cascade above) and the next two steps is in location 2. In each case the only diffusing species is the communicating species, and the relevant models can be easily described by a simple expansion of the model considered above. We therefore do not explicitly describe these equations. A third case also considered is when the first and third steps are in location 1 and the second step is in location 2. This involves two communicating species. Again, this is described in an analogous manner.

Cases studied: We have examined a separated two step cascade, implemented as described above: the first stage is in one spatial location and the second stage is in the second spatial location, with the modified species at stage 1 being diffusible in the entire domain. We also study special cases of this scenario when the first stage operates in the ultrasensitive enzymatic regime, and the second stage operates in the mass-action kinetic regime, and this is implemented simply by an appropriate choice of kinetic parameters. In the case of the three stage cascade, a similar model of a cascade with 3 stages is studied. Here we consider different spatial designs as discussed in the text (see Fig. 3). This corresponds to localizing the entities involved in the stages in either of the compartments (implemented exactly as above) with the communicating species diffusing in the spatial domain.

Multiple Modification of Substrate. We now describe a spatial model of a 2-site ordered modification of substrate X. Here the modification of X to X^* is mediated by the kinase K1 and phosphatase P1, and the modification of X^* to X^{**} is mediated by the kinase K2 and the phosphatase P2. Note that, in an ordered multisite modification, there is a specific order to the modifications, in contrast to a random modification mechanism.

We will present a model which depicts the localization/compartmentalization of the two stages of this modification sequence, a scenario depicted in Fig. S1. In order to discuss this model, we first present a general spatial model of this two ordered site modification system. This is described by the equations:

$$
\begin{aligned}
\frac{\partial[X]}{\partial t} &= -k_1[X][K1] + k_{-1}[XK1] + k_4[X^*P1] + D_X\frac{\partial^2[X]}{\partial\theta^2} \\
\frac{\partial[X^*]}{\partial t} &= -k_3[X^*][P1] + k_{-3}[X^*P1] + k_2[XK1] - k_5[X^*][K2] + k_{-5}[X^*K2] + k_8[X^{**}P2] + D_{X^*}\frac{\partial^2[X^*]}{\partial\theta^2} \\
\frac{\partial[X^{**}]}{\partial t} &= k_7[X^{**}][P2] - k_{-7}[X^{**}P2] + k_6[X^*K2] + D_{X^{**}}\frac{\partial^2[X^{**}]}{\partial\theta^2} \\
\frac{\partial[K1]}{\partial t} &= -k_1[X][K1] + k_{-1}[XK1] + k_2[XK1] + D_{K1}\frac{\partial^2[K1]}{\partial\theta^2} \\
\frac{\partial[P1]}{\partial t} &= -k_3[X^*][P1] + k_{-3}[X^*P1] + k_4[X^*P1] + D_{P1}\frac{\partial^2[P1]}{\partial\theta^2} \\
\frac{\partial[K2]}{\partial t} &= -k_5[X^*][K2] + k_{-5}[X^*K2] + k_6[X^*K2] + D_{K2}\frac{\partial^2[K2]}{\partial\theta^2} \\
\frac{\partial[P2]}{\partial t} &= -k_7[X^{**}][P2] + k_{-7}[X^{**}P2] + k_8[X^{**}P2] + D_{P2}\frac{\partial^2[P2]}{\partial\theta^2} \\
\frac{\partial[XK1]}{\partial t} &= k_1[X][K1] - k_{-1}[XK1] - k_2[XK1] + D_{XK1}\frac{\partial^2[XK1]}{\partial\theta^2} \\
\frac{\partial[X^*P1]}{\partial t} &= k_3[X^*][P1] - k_{-3}[X^*P1] - k_4[X^*P1] + D_{X^*P1}\frac{\partial^2[X^*P1]}{\partial\theta^2} \\
\frac{\partial[X^*K2]}{\partial t} &= k_5[X^*][K2] - k_{-5}[X^*K2] - k_6[X^*K2] + D_{X^*K2}\frac{\partial^2[X^*K2]}{\partial\theta^2} \\
\frac{\partial[X^{**}P2]}{\partial t} &= k_7[X^{**}][P2] - k_{-7}[X^{**}P2] - k_8[X^{**}P2] + D_{X^{**}P2}\frac{\partial^2[X^{**}P2]}{\partial\theta^2}
\end{aligned}
\tag{3}
$$

The above model is simply a description of all the kinetic steps involved in the modification sequence, incorporating the diffusion of each species. The substrate species are X, X^*, X^{**}, while the relevant complexes are XK1, X^*P1, X^*K2 and $X^{**}P2$. The enzymes are K1 and P1 (first modification step) and K2 and P2 (second modification step). The forward association rate constants of the relevant enzyme to substrate are k_1, k_3, k_5 and k_7, the dissociation rate constants of the relevant enzyme substrate complexes are k_{-1}, k_{-3}, k_{-5} and k_{-7} and the corresponding catalytic constants are k_2, k_4, k_6 and k_8. The diffusion coefficients are $D_X, D_{K1}, D_{XK1}, D_{X^*}, D_{P1}, D_{X^*P1}, D_{X^*K2}, D_{X^{**}}, D_{K2}, D_{X^{**}P2}$ and D_{P2}, where the subscript denotes the species under consideration.

We focus on the effects of localization in the cascade. This is described in the model as follows. All species relevant to the first modification (and demodification) are in the first location, while those relevant to the second modification (and demodification) are present in the second location (see Fig. S1). All these species are regarded as non-diffusible. The initial conditions reflect the spatial localization of these components. Since these species are non-diffusible they remain localized in the relevant compartments. The only species which is diffusible is X^*. Thus the model describes a situation which is an analogue of

the two step cascade considered above: the spatial separation of two stages of this sequence with the common species diffusing from one location to the other to effect the communication. The only difference with the 2-step cascade is that the modified species acts as a substrate in the second stage.

Cases studied: The basic case studied involved unmodified substrate, K1 and P1 in the first compartment, while the enzymes K2 and P2 are in the second compartment. The modified form X^* diffuses everywhere in the spatial domain. The unmodified and doubly modified forms X and X^{**} are non-diffusible, and thus X^{**} remains in the second compartment. Some additional scenarios were also studied. In one case, we examined the case where the phosphatase is common for both steps. Thus in this case, we have exactly the same set up as above, except that the phosphatase in the second compartment is also P1 (at a possibly different concentration). Note that the P1 in each compartment remains in the relevant compartment. Then, we considered a scenario where all modifications occur in one compartment but X^{**} can diffuse out. This amounts to localizing all elements in the first compartment, but allowing X^{**} to be diffusible. A final case which is briefly studied in section 2.6 below involves the scenario where the same kinase K effects both modifications and the same phosphatase P effects reverse modifications. Here K (and corresponding kinase complexes) is localized in compartment 1, P (and corresponding phosphatase complexes) is localized in compartment 2 and the unmodified substrate X and fully modified substrate X^{**} diffuse in the spatial domain.

Phosphorelay. We now consider a different kind of modification sequence: a phosphorelay. We describe a spatial model of 4 step phosphorelay with phosphatases at each step. We first present a general model which allows the output of any of the stages to be the communicating species. All other species are assumed non-diffusible. The 4 step phosphorelay is described by the following equations:

$$
\begin{aligned}
\frac{\partial[X1]}{\partial t} &= -k_s[X1][K1] + k_2[X1^*X2] + k_{p2}[X1^*P1] \\
\frac{\partial[X1^*]}{\partial t} &= k_s[X1][K1] - k_1[X1^*][X2] + k_{-1}[X1^*X2] - k_{p1}[X1^*][P1] + k_{-p1}[X1^*P1] + D_{X1^*}\frac{\partial^2[X1^*]}{\partial\theta^2} \\
\frac{\partial[X2]}{\partial t} &= -k_1[X1^*][X2] + k_{-1}[X1^*X2] + k_4[X2^*X3] + k_{p4}[X2^*P2] \\
\frac{\partial[X2^*]}{\partial t} &= -k_3[X2^*][X3] + k_{-3}[X2^*X3] - k_{p3}[X2^*][P2] + k_{-p3}[X2^*P2] + k_2[X1^*X2] + D_{X2^*}\frac{\partial^2[X2^*]}{\partial\theta^2} \\
\frac{\partial[X3]}{\partial t} &= -k_3[X2^*][X3] + k_{-3}[X2^*X3] + k_{p6}[X3^*P3] + k_6[X3^*X4] \\
\frac{\partial[X3^*]}{\partial t} &= -k_5[X3^*][X4] + k_{-5}[X3^*X4] + k_4[X2^*X3] - k_{p5}[X3^*][P3] + k_{-p5}[X3^*P3] \\
&\quad + D_{X3^*}\frac{\partial^2[X3^*]}{\partial\theta^2} \\
\frac{\partial[X4]}{\partial t} &= -k_5[X3^*][X4] + k_{-5}[X3^*X4] + k_{p8}[X4^*P4] \\
\frac{\partial[X4^*]}{\partial t} &= -k_{p7}[X4^*][P4] + k_{-p7}[X4^*P4] + k_6[X3^*X4] + D_{X4^*}\frac{\partial^2[X4^*]}{\partial\theta^2} \\
\frac{\partial[X1^*X2]}{\partial t} &= k_1[X1^*][X2] - (k_{-1} + k_2)[X1^*X2] \\
\frac{\partial[X2^*X3]}{\partial t} &= k_3[X2^*][X3] - (k_{-3} + k_4)[X2^*X3] \\
\frac{\partial[X3^*X4]}{\partial t} &= k_5[X3^*][X4] - (k_{-5} + k_6)[X3^*X4] \\
\frac{\partial[X1^*P1]}{\partial t} &= k_{p1}[X1^*][P1] - (k_{-p1} + k_{p2})[X1^*P1] \\
\frac{\partial[X2^*P2]}{\partial t} &= k_{p3}[X2^*][P2] - (k_{-p3} + k_{p4})[X2^*P2] \\
\frac{\partial[X3^*P3]}{\partial t} &= k_{p5}[X3^*][P3] - (k_{-p5} + k_{p6})[X3^*P3] \\
\frac{\partial[X4^*P4]}{\partial t} &= k_{p7}[X4^*][P4] - (k_{-p7} + k_{p8})[X4^*P4] \\
\frac{\partial[P1]}{\partial t} &= -k_{p1}[X1^*][P1] + (k_{-p1} + k_{p2})[X1^*P1] \\
\frac{\partial[P2]}{\partial t} &= -k_{p3}[X2^*][P2] + (k_{-p3} + k_{p4})[X2^*P2] \\
\frac{\partial[P3]}{\partial t} &= -k_{p5}[X3^*][P3] + (k_{-p5} + k_{p6})[X3^*P3] \\
\frac{\partial[P4]}{\partial t} &= -k_{p7}[X4^*][P4] + (k_{-p7} + k_{p8})[X4^*P4]
\end{aligned}
\tag{4}
$$

The above model is simply a detailed depiction of all the elementary kinetic steps of a 4-stage phosphorelay, incorporating potential diffusion of the output of each stage of the relay (a 2-stage phosphorelay is depicted in Fig. S1). In the above model, the substrate species are X1, X2, X3, X4,

$X1^*, X2^*, X3^*$ and $X4^*$. The substrate complexes are $X1^*X2, X2^*X3$ and $X3^*X4$. The phosphatase substrate complexes are $X1^*P1, X2^*P2, X3^*P3$ and $X4^*P4$. The enzymes are K1 (the kinase for the first stage), and the phosphatases for the four stages are P1, P2, P3 and P4 respectively. The forward binding rate constants are k_s, k_1, k_3, k_5 (for the relevant forward modifications of each stage) and $k_{p1}, k_{p3}, k_{p5}, k_{p7}$ (for the reverse modifications of each stage). The dissociation/unbinding rate constants are $k_{-1}, k_{-3}, k_{-5}, k_{-p1}, k_{-p3}, k_{-p5}, k_{-p7}$ and the catalytic rate constants are $k_2, k_4, k_6, k_{p2}, k_{p4}, k_{p6}$ and k_{p8}. The diffusion coefficients of the substrate species are $D_{X1^*}, D_{X2^*}, D_{X3^*}$ and D_{X4^*}, where the subscript denotes the species under consideration. The first step of the phosphorelay is assumed to occur through mass action kinetics.

The above model is a simple model of a phosphorelay, where each elementary step is modelled by mass action kinetics; the binding/unbinding of the species is described explicitly. The main difference between this model and that of the cascade arises in the fact when the output at one stage (say $X1^*$) transfers a phosphate group to a species in the next stage (say $X2$), it gets converted back (to $X1$).

As before, we will consider different scenarios where some steps are localized in one location and other steps are localized in the other location. For instance a scenario where the first two steps are in one spatial location and the last two are in a second location, is described in the model by having $X2^*$ be the only diffusible species, and all other components be non-diffusible and initially localized in their respective compartments. The relevant communicating species is the sole diffusing species in such cases and all other species remain localized in their respective compartments. Thus such a model describes a phosphotransfer mechanism with spatial localization.

A two step phosphotransfer model is obtained by considering only the first two steps in the model above. Making $X1^*$ the only diffusible species and localizing the first stage in one location and the second stage in another location results in the two step phosphotransfer model with compartmentalization (see Fig. S1).

Cases studied: The basic cases we studied were two-stage and four-stage phosphorelays, with compartmentalization. This was done by localizing the elements of the corresponding stages in the appropriate compartments, and having the communicating species diffuse in the spatial domain. In the case of the two stage phosphorelay, the first stage entities are in compartment 1 and the second stage entities are in compartment 2, with the species $X1^*$ diffusing in the spatial domain. In the case of a four stage phosphorelay, there are multiple ways to partition the cascade between the two compartments, but again this is implemented in exactly the same way: the first part of the cascade is in location 1, the second part of

the cascade is in location 2, with the communicating species diffusing everywhere in the spatial domain. We also consider some variants of this basic scenario: one was where the phosphatase of the last stage could act as a kinase of the first stage. This phosphatase was always present only in compartment 2, and the model was refined to allow it to modify $X1$ to $X1^*$ at this location if $X1$ was present here. This was studied for both the two stage and four stage phosphorelay.

1.2 Open cascade

For completeness, we also consider open models of modification sequences. For instance, we consider a 3 step modification sequence (assumed irreversible, for simplicity: reversible analogues have also been studied). Here $X1$ is modified to $X2$ which is modified to $X3$. The only difference here is that there is a constant production of $X1$ and a removal of $X3$, proportional to its concentration. This is described by the model

$$\begin{aligned}
\frac{\partial[X1]}{\partial t} &= k_o - k_s[S][X1] \\
\frac{\partial[X2]}{\partial t} &= k_s[S][X1] - k_2[X2] + D_{X2}\frac{\partial^2[X2]}{\partial\theta^2} \\
\frac{\partial[X3]}{\partial t} &= k_2[X2] - k_d[X3]
\end{aligned} \tag{5}$$

The signal S enters the chain of reactions between X1 and X2, catalyzing the conversion of $X1$ to $X2$. k_o is the generation term for X1 (and is non-zero only in the first compartment) and k_s is the rate constant associated with the signal converting X1 to X2. k_2 is the rate constant associated with the conversion of X2 to X3 (this occurs only in the second compartment) and k_d is the degradation constant for X3. We will assume that $X2$ is the communicating species and that $X1$ is in the first location and $X3$ is in the second location. D_{X2} is the diffusion coefficient for X2. It should be noted that by making $X2$ non-diffusible and by localizing all species in the same location, we recover the ODE model of this modification sequence (with input and removal). All reactions are described by mass-action kinetics for simplicity.

One can consider a minor variation of the above structure, where the signal is associated with the

conversion from $X2$ to $X3$. This is described by the model

$$\begin{aligned}\frac{\partial[X1]}{\partial t} &= k_o - k_1[X1] \\ \frac{\partial[X2]}{\partial t} &= k_1[X1] - k_s[S][X2] + D_{X2}\frac{\partial^2[X2]}{\partial\theta^2} \\ \frac{\partial[X3]}{\partial t} &= k_s[S][X2] - k_d[X3]\end{aligned} \tag{6}$$

Here, k_o is the generation term for X1 (present only in compartment 1) and k_1 is the rate constant associated with the conversion of X1 or production of X2. k_s is the rate constant for X2 being converted to X3 by the signal (this happens only in compartment 2) and k_d is the degradation constant for X3. D_{X2} is the diffusion coefficient for X2.

Cases studied: The cases we have studied involve $X1$ in compartment 1, $X3$ in compartment 2, and $X2$ diffusing everywhere. In one case, the signal is associated with the conversion of $X1$ to $X2$ (this happens only in compartment 1) and in the other case, the signal is associated with the conversion of $X2$ to $X3$ (this happens only in compartment 2).

2 Analysis of models

2.1 Cascades

We first consider a two step enzymatic cascade for concreteness. Note that here X^* is the communicating species between the two compartments and also the only diffusible species. By adding all the equations of all the species, we find that all kinetic terms cancel out leaving, at steady state,

$$\frac{\partial^2[X^*]}{\partial\theta^2} = 0$$

This shows that this species has a spatially uniform profile. We now deduce some facts based on this.

Spatial separation can result in reduction of the output of the cascade:

We start by noting that the steady state of the cascade corresponds to the standard kinetic equations (i.e. those resulting from the ODEs) in each compartment, along with the conservation condition. The conservation of total substrate implies that $L_1([X] + [XK1] + [X^*P1] + [X^*Y]) + L[X^*] = L_1X_{tot}$. Note that X_{tot} corresponds to the total concentration of X species present initially and that L_1X_{tot} hence

corresponds to the total amount of this species in the system. Similarly, $[Y] + [X^*Y] + [Y^*] + [Y^*P2] = Y_{tot}$. Y_{tot} corresponds to the total concentration of Y species present initially and that $L_1 Y_{tot}$ hence corresponds to the total amount of this species in the system. The Y species remains localized in the second compartment, and hence the sum of concentrations of all the species involving Y is constant. In the above, L_1 corresponds to the size of the compartments (assumed equal) and L corresponds to the size of the overall domain. Clearly $L > 2L_1$ if the two patches are disjoint and separated (the case we study of spatial cascades). $L = L_1$ corresponds to the situation where the two patches are coincident. Writing $L = L_1 + L_e$ we see from the conservation equation above, that in effect the available total amount of X species in compartment 1 is reduced by a factor $L_e[X^*]$. For simplicity to start with, we will assume that dephosphorylation in the second step occurs via mass action kinetics.

We will approach this in two stages. Suppose there was no retroactivity (i.e. the phosphorylation in the second stage occurred via mass action kinetics). Then, we see that the conservation equation for species X results in $L_1([X] + [XK1] + [X^*P1]) + L[X^*] = L_1 X_{tot}$. In other words $[X] + [XK1] + [X^*] + [X^*P1] \leq X_{tot}$: the total concentration of X species in the first compartment is reduced due to its spreading in the domain.

Now note that the steady state of the first stage is determined by the steady state of the ODE model for this stage (note that at steady state $[X^*]$ is uniform, and the flux out of the compartment is zero) with an appropriate reduced effective total amount of X species in compartment 1 (i.e. a reduced effective X_{tot})), accounting for the leakage of X^*. We now show that at steady state in the ODE kinetic model $d[X^*]/dX_{tot} > 0$. Showing this amounts to showing that the steady state of X^* which is obtained when it leaks out is less than when all the reactions occur in the same compartment. We focus on the ODE kinetic model. Clearly this is the case for small X_{tot}, so if this condition were violated, we must require $d[X^*]/dX_{tot} = 0$ for some value of parameters. Now analyzing the model of the first level of the cascade, we see from conservation of enzymes that $[XK1] = \alpha_1 K_{tot}[X]/(1 + \alpha[X])$, $[X^*P1] = \beta_1 P1_{tot}[X^*]/(1 + \beta[X^*])$ for suitable constants $\alpha, \alpha_1, \beta, \beta_1$. Furthermore the concentrations of these complexes are proportional to each other at steady state. Now if $d[X^*]/dX_{tot} = 0$, then it follows immediately that $d[X^*P1]/dX_{tot} = 0$ and from above that $d[XK1]/dX_{tot} = 0$ (proportionality of complexes). It then follows that $d[X]/dX_{tot} = 0$. These conditions violate the conservation of species, and hence we conclude for a single covalent modification cycle $d[X^*]/dX_{tot} > 0$. Now if we consider this in light of a spatial cascade with no retroactivity, we find that the spreading of X^* in the domain reduces the total X species in compartment 1. This immediately means that X^* is reduced as a result, and since the

kinetics in the second cycle is mass action, it means that $[Y^*]$ is also reduced (it being an increasing function of the concentration of $[X^*]$).

We now examine a situation where the phosphorylation in the second cycle is not necessarily mass action (the dephosphorylation is still assumed to occur via mass action kinetics). Here we employ conservation of species Y to impose $[Y] + [Y^*] + [X^*Y] = Y_{tot}$. Now the steady state for the second cycle means $\gamma_1[Y^*] = \gamma_2[X^*Y] = \gamma_3([X^*])([Y])$ for suitable constants $\gamma_1, \gamma_2, \gamma_3$. From this and the fact that the steady state concentration of the complex X^*Y is proportional to the product of concentrations of X^* and Y, we can infer that at steady state, the functional relationship between $[Y^*]$ and $[X^*]$ is of the form

$$\begin{aligned}[Y^*] &= \frac{Y_{tot}[X^*]}{a_1 + b_1[X^*]} \\ [X^*Y] &= \frac{aY_{tot}[X^*]}{a_1 + b_1[X^*]}\end{aligned} \tag{7}$$

Here a, a_1, b_1 are constants.

Now in this case, the steady state for $[X^*]$ is governed by the same kinetic equations in the first location, along with the modified conservation condition
$L_1([X] + [XK1] + [X^*P1] + [X^*Y]) + L[X^*] = L1X_{tot}$.

We now reason as follows. In the ODE model of the two step cascade, we see (under the conditions above) that $d[X^*]/dX_{tot} > 0$. Clearly this is the case for small X_{tot} so if this condition were violated, we must require $d[X^*]/dX_{tot} = 0$ for some value of parameters. We show that this is not possible. To do this we follow the exact same procedure above. We note that in the conservation relationship for species X, there is an extra term corresponding to the concentration of the complex $[X^*Y]$, which as noted above is related to X^* in the manner described. Thus if $d[X^*]/dX_{tot} = 0$, then it automatically follows that the derivative of this term with respect to X_{tot} is also zero. Thus the above argument carries through exactly. It is impossible to satisfy the conservation condition if $d[X^*]/dX_{tot} = 0$ at steady state. Thus $d[X^*]/dX_{tot} > 0$.

Now for the distributed system at steady state, the species of tier-1 satisfies the same steady state equation as the ODEs with a reduced X_{tot} (corresponding the extra X^* in the medium: compare the conservation conditions of the co-localized cascade, and the distributed cascade). Therefore at steady state $[X^*]$ is reduced when compared to the situation where all species are localized together. From above it immediately follows that the same is true for $[Y^*]$. This shows how the separation of steps leads to a reduction in the output of the cascade.

Retroactivity. The above analysis can be used to examine the amount of X species contained in the

downstream complex X^*Y which is a measure of the retroactivity. We see from the above analysis that the $[X^*Y]$ is related to the $[X^*]$ via a monotonic function. Since the separation leads to a reduction in $[X^*]$ (relative to the ODEs), we find that the $[X^*Y]$ concentration is also reduced. In other words, the separation leads to a reduction in the retroactive effect.

The case where dephosphorylation of the second stage does not occur in the mass action regime. In the above analysis we considered the case where the dephosphorylation of the second stage occurred via mass action kinetics. We now relax that assumption. In this case, we start our analysis of the ODE model from the second stage of our cascade. We show that at steady state $d[Y^*]/dX_{tot} > 0$. Now clearly this is the case for small X_{tot}, and so if this condition were violated, then at some value of X_{tot}, $d[Y^*]/dX_{tot} = 0$. Now at steady state in the second cycle, we have

$$\begin{aligned} [Y^*P2] &= \frac{P2_{tot}[Y^*]}{c_1 + d_1[Y^*]} \\ e_1[X^*Y] &= f_1[Y^*P2] \end{aligned} \tag{8}$$

and $[X^*Y] = \alpha_1([X^*])([Y])$ where $\alpha_1, c_1, d_1, e_1, f_1$ are all positive constants. Now suppose $d[Y^*]/dX_{tot} = 0$, it immediately follows that $d[Y^*P2]/dX_{tot} = 0$ and hence that $d[X^*Y]/dX_{tot} = 0$ from above. Now since $[Y] + [Y^*] + [X^*Y] + [Y^*P2] = Y_{tot}$, it follows that $d[Y]/dX_{tot} = 0$. This, along with the fact that $d[X^*Y]/dX_{tot} = 0$, shows that $d[X^*]/dX_{tot} = 0$. The rest of the argument is identical to the cases above, indicating that this is an impossibility. Therefore we have $d[Y^*]/dX_{tot} > 0$, and from above $d[X^*Y]/dX_{tot} > 0$. Now exactly as before, we note that the the steady state of the distributed cascade satisfies the same equations as the ODEs but with a reduced X_{tot}. This implies both a reduction in output, as well as a reduction in the retroactivity, just as before.

Buffering against dilution. The above analysis also provides insights into how the dilution effects can be buffered against in cascades. We see that the dilution effect occurs through X^* spreading in the medium. There are different ways to reduce this effect. One way is to reduce the length of the medium. A second way, also seen from above, is to increase phosphatase $P1$ concentration. This leads to a reduction in $[X^*]$. Now a low $[X^*]$ will also result in a lower amount of dilution in the medium with the result that the effective total amount of X in location 1 will be modified only slightly. Thus the characteristics of the cascade are affected in only a minor way. While this of course involves operating the cascade in a regime of relatively low $[X^*]$, Table 1 shows how the effect of dilution in both absolute and relative terms is buffered against.

To complement this, we perform some basic analytical calculations to illustrate the main points. We

will assume negligible retroactivity, for simplicity, and focus on a single stage of the cascade. We note that we will be examine scenarios of high $P1$ concentration: this means that the free $P1$ concentration practically equals the total $P1$ concentration. For simplicity, suppose the first step of the cascade occurs through mass action kinetics. Then the functional relationship between the variables at steady state are given by

$$\begin{aligned} a_1[X][K1] &= b_1[X^*][P1] \\ L_1([X]+[X^*])+L_e[X^*] &= L_1 X_{tot} \end{aligned}$$

where $L = L_1 + L_e$, a_1, b_1 are constants. Here $K1, P1$ equal $K1_{tot}, P1_{tot}$ respectively. This results in a steady state

$$[X^*] = \frac{X_{tot}}{1 + L_e/L_1 + b_1 P1_{tot}/a_1 K1_{tot}} \tag{9}$$

The dilution effect is contained in the term L_e/L_1. We see in the above equation that when the last term in the denominator is large, it can dwarf the second term. The ratio of the steady state in the distributed cascade to that of the colocalized cascade ($L_e = 0$) is given by

$$R = \frac{1 + b_1 P1_{tot}/a_1 K1_{tot}}{1 + L_e/L_1 + b_1 P1_{tot}/a_1 K1_{tot}} \tag{10}$$

and this ratio approaches 1 as $P1_{tot}$ is increased. This explains the assertion that it is possible to buffer against dilution, even in relative terms.

We can extend this analysis even when the kinetics is not in the mass action regime. If we focus on tthe functional relationships between the variables, we have at steady state

$$\begin{aligned} [X^*P1] &= \gamma_1 P1_{tot}[X^*] \\ \gamma_2[XK1] &= \gamma_3[X^*P1] \\ [XK1] &= \gamma_4 K1_{tot}[X]/(1+\gamma_4[X]) \\ L_1 X_{tot} &= L1([X]+[XK1]+[X^*P1]+[X^*])+L_e[X^*] \end{aligned} \tag{11}$$

where all the γ terms are constants. Eliminating $[X^*]$ and writing the equation in terms of $[X]$, results in an equation of the form

$$[X] + \gamma_4 \frac{K1_{tot}[X]}{(1+\gamma_4[X])} + \beta_2 \frac{K1_{tot}[X]}{P1_{tot}(1+\gamma_4[X])} + \beta_2 \frac{L_e}{L_1} \frac{K1_{tot}[X]}{P1_{tot}(1+\gamma_4[X])} = X_{tot} \tag{12}$$

where the various β terms are constants. Even without solving this equation we see that the dilution effect (contained in the term L_e/L_1) is actually reduced by the presence of large $P1_{tot}$. X^* can be obtained from X via an equation independent of L_e, and is also hence buffered against.

Cascade with one step in the Goldbeter-Koshland regime. In the text we mentioned that one way to propagate the effects of a Goldbeter-Koshland switch spatially, is to keep that step localized, and have that propagated by a communicating step involving species I and I^* with the output (X^*) of the Goldbeter-Koshland module regulating the conversion of I to I^* through mass-action kinetics. The kinetics for the species I, I^* can be written as

$$\begin{aligned} \frac{\partial [I]}{\partial t} &= -k_{f1}[X^*][I] + k_{r1}P_0[I^*] \\ \frac{\partial [I^*]}{\partial t} &= k_{f1}[X^*][I] - k_{r1}P_0[I^*] + D_{I^*}\frac{\partial^2 [I^*]}{\partial \theta^2} \end{aligned} \tag{13}$$

Here I is localized in region 1 and so is the phosphatase for this stage P_0. In this case, X^* is not taken up in the downstream reaction and so it exhibits a switch like response to its input, since the behaviour of X^* is determined by ODEs for that layer of the cascade. $[X^*]$ is a parameter in the equations above. Further, the communicating layer (I, I^*) can be regarded as the first step of a cascade similar to what we have studied in the paper, and the switch behaviour is already present in the input to this layer. Thus, the switch effect is propagated in the cascade, though dilution via the diffusing species reduces the amplitude, relative to the situation where all steps are co-localized. Overall, a switch behaviour is seen in the spatially distributed cascade.

Transient response of cascades: effect of pulse duration: In the text we examined the response of three step cascades to pulse inputs, examining the effects of diffusivity of the communicating species, as well as the patch size. We briefly examine the effect of pulse duration here, for fixed diffusivity of communicating species. Increasing pulse duration increases the transient peak concentration and results in a clear plateau in the transient response of the output (Fig. S3(b)). In general, the sensitivity to pulse duration depends on the pulse duration relative to kinetic time scales of the cascade and the time scale of diffusion of the communicating species.

2.2 Multisite modification and phosphotransfer

Multisite Modification. We briefly examine aspects of the multisite modification. Again, since X^* is the

only species which is diffusing, we find by adding all the equations that at steady state

$$\frac{\partial^2[X^*]}{\partial\theta^2} = 0$$

In other words the concentration of X^* is uniform in the domain. The conservation condition for substrate is altered by the fact that X^* spreads in the medium. The equation becomes
$L_1([X] + [XK1] + [X^*P1] + [X^*K2] + [X^{**}] + [X^{**}P2]) + L[X^*] = L_1X_{tot}$.

We will show that in the ODE model of the two site modification $[dX^{**}]/dX_{tot} > 0$. This can be seen by examining the two cycles sequentially. Firstly we see that by applying the conservation conditions for all the enzymes we have $[P1] = P1_{tot}/(1 + \gamma_1[X^*])$ $[K1] = K1_{tot}/(1 + \gamma_2[X])$,
$K2 = K2_{tot}/(1 + \gamma_3[X^*])$, $P2 = P2_{tot}/(1 + \gamma_4[X^{**}])$, where γ_i are constant. Furthermore, all complex concentrations are simply proportional to the product of those of the corresponding free enzyme and substrate.

We note that $d[X^{**}]/dX_{tot} > 0$, for small X_{tot}. Suppose the inequality does not hold, we must require that $d[X^{**}]/dX_{tot} = 0$ at some parameter value. From an analysis of the second covalent modification cycle, since the concentrations of the two complexes are proportional at steady state, and the fact that each complex is related to the substrate concentration as a function of the form $a[S]/(1 + b[S])$, we immediately see that $d[X^{**}P2]/dX_{tot} = 0$, $d[X^*K2]/dX_{tot} = 0$. From this it follows that $d[X^*]/dX_{tot} = 0$.

Now, we use this and repeat the same analysis in the first cycle, to find that the derivative of concentrations of all substrate and complex species with respect to X_{tot} is zero. This leads to a contradiction since this violates the conservation condition for substrate species. This shows therefore that $d[X^{**}]/dX_{tot} > 0$. Now if we contrast the spatially segregated model of the multisite modification model to that where all modifications occur together, we see that at steady state the formal kinetic equations satisfied in both cases is the same. The only difference arises in the conservation conditions. The steady state for the spatially distributed model corresponds to the steady state of a model with co-localized modifications (i.e. an ODE model) with a reduced X_{tot}. Since $d[X^{**}]/dX_{tot} > 0$, we find that the spatially distributed modification results in reduced $[X^{**}]$.

The variation of concentration and total amount of X^* with domain size: basic case We now turn to a different aspect of multisite modification. We examine both the concentration of X^* and the total amount of this species in the situation when all modifications occur in the same location (patch of size L_1) and when the modifications are separated as examined above, also studying the effect of varying the overall

domain size. For simplicity, and to get some intuition, we will assume that all modifications occur via mass action kinetics (i.e. effectively very large catalytic constants for all modifications). In this case we have at steady state $[X^*]/[X] = \alpha K1_{tot}/P1_{tot}$ and $[X^{**}]/[X^*] = \beta K2_{tot}/P2_{tot}$, where α, β are the equilibrium constants for the two reactions. Now the conservation condition reads
$L_1([X] + [X^{**}]) + L[X^*] = L_1 X_{tot}$. From this it simply follows that

$$[X^*] = \frac{L_1 X_{tot}}{L_1(P1_{tot}/(\alpha K1_{tot}) + \beta K2_{tot}/P2_{tot}) + L}$$
$$[X^{**}] = \frac{\beta L_1 X_{tot} K2_{tot}/P2_{tot}}{L_1(P1_{tot}/(\alpha K1_{tot}) + \beta K2_{tot}/P2_{tot}) + L}$$

It is clear from above that steady state concentrations of X^* and X^{**} are decreasing functions of L. Hence the concentration of these species in the separated case is also less than the co-localized case ($L = L_1$), as can also be expected from the previous discussion. Now if we consider the total amount of X^* species in the domain, that is given by $L[X^*]$, we find that this is a function which actually increases with L. We thus see that separated modification and increased separation does indeed decrease the doubly modified phosphoform concentration but in fact increases the total amount of phosphoform species X^* in the domain.

The effect of domain size on the total amount of X^*: the general case. We will now show the behaviour of the total amount of X^* in the domain increasing with domain length L, occurs even when the kinetics is far from mass action. To do this we note

(1) All relevant enzyme-substrate complex concentrations, can be related to their substrate in the form $[ES] = a[S]/(1 + b[S])$ where a,b are constants related to kinetic parameters. Note that the enzymes in the different modification stages are different.

(2) The steady state for the distributed cascade, involves the steady state for each set of modifications at their relevant locations. Considering the two stages, we have equations of the form
$a_1[X^*]/(1 + b_1[X^*]) = a_2[X^{**}]/(1 + b_2[X^{**}])$ and $a_3[X]/(1 + b_3[X]) = a_4[X^*]/(1 + b_4[X^*])$.

(3) By differentiating these equations with respect to L (or inverting them and differentiating them), we see that the derivative of X, X^*, X^{**} all have the same sign, and noting point (1), so do the derivatives of all relevant complexes.

(4) Now the conservation condition states that
$L_1([X] + [XK1] + [X^*P1] + [X^*K2] + [X^{**}] + [X^{**}P2]) + L[X^*] = L_1 X_{tot}$. Suppose that the derivative of all the relevant concentrations with respect to L were positive. Then we find that the conservation condition would be impossible to satisfy. Thus we must have that the derivative of all these

concentrations must be negative. Then, by differentiating the conservation condition with respect to L, we have $d/dL(L[X^*]) > 0$, which demonstrates the point.

Common Phosphatase. It is clear to see in the case of multisite modification with shared (i.e. common) phosphatase, that a situation of separated modifications will result in all the X species in the second domain to be converted to the unmodified form X. Further, at steady state the concentration of X^* (which is uniform in the domain) is 0. This is simply seen by considering the second location. Firstly we know from above that the concentration of X^* is spatially uniform. Now in the second location, by examining the kinetics of conversion we see that all available X^* is converted to X. In other words, by examining the steady state condition for X, we see that $[X^*] = 0$ (since there is nothing to remove X and what is produced is produced via X^*). From this it follows that $[X^{**}] = 0$ and in fact the only species in location 2 is X. In fact all the substrate species ends up as X in the second location. This is true irrespective of the model parameters. In such a situation, an extra mechanism would be needed to transfer the X back to the original location.

Phosphorelay. We briefly discuss a couple of aspects of the phosphorelay mechanism. We asserted that a 2 step separated model of the phosphorelay would result in 0 concentration of the output at steady state. We therefore consider a two step phosphorelay mechanism. Again we find similar to before that the spatial concentration profile of the communicating species $X1^*$ is uniform at steady state. This is obtained by adding all the equations of the species. Now, we notice that owing to the phosphotransfer mechanism, $X1^*$ is converted to $X1$ at the second location. By examining the equation for $X1$ at the second equation at steady state, we find that $[X1^*] = 0$ at steady state. This is because $X1$ is produced by $X1^*$ and not removed by any other mechanism. Therefore $[X1^*] = 0$ at steady state, from which it follows that $[X2^*] = 0$. Naturally $[X2^*]$ may transiently increase from 0. We see a reasoning very similar to the situation above. Again, this conclusion does not depend on model parameters.

Finally, we briefly examine a 4 step phosphorelay, where the phosphatase of the final step is a bifunctional kinase (capable of triggering the phosphorelay). We see that if the phosphorelay is separated after the first step (i.e. the communicating species is $X2^*$ or $X3^*$) then by exactly the same reasoning as above, we find that $[X4^*]$ at steady state is 0. Since the phosphatase of the final stage is the second location, it cannot trigger the conversion of $X1$ to $X1^*$. If however the communicating species is $X1^*$ then this is not necessarily the case: this is because the bifunctional kinase can effect a conversion from $X1$ (created in the second location) back to $X1^*$. Naturally, this pre-supposes the fact that the bifunctional kinase is capable of functioning as a kinase in the second location. For the same reason, if we have a two

stage phosphorelay, with $X1^*$ being the communicating species, it is possible to have a non-zero steady state of $X1^*$ and $X2^*$. This justifies what we mentioned in the text.

2.3 Irreversible cascade with inflow and outflow

We now examine the 3 species irreversible cascade with inflow and outflow. By placing the entire cascade in one location, we find that at steady state, by adding all the equations of species, $[X3] = k_o/k_d$. This shows how at steady state the output of the cascade recovers to pre-stimulus values (it is independent of S), exhibiting an adaptive response. We now consider spatial models of such a cascade. For specificity, we consider a situation where $X2$ is the diffusing species, and the signal mediates the conversion of $X2$ to $X3$. Now by adding all the equations and integrating over the full domain, we find that $k_o L_1 = k_d \int_0^{L_1} [X3] d\theta$. This shows that the spatially averaged concentration of the output of the cascade, X3 is in fact constant at a level independent of the stimulus, at steady state.

In order to obtain the steady state for $[X3]$, we need to find the steady state for $[X2]$. The steady state for $[X2]$ is governed by

$$\begin{aligned} k_o + D_{X2}\frac{\partial^2[X2]}{\partial\theta^2} &= 0, \quad 0 \le \theta < L_1/2 \\ D_{X2}\frac{\partial^2[X2]}{\partial\theta^2} &= 0, \quad L_1/2 \le \theta < (L-L_1)/2 \\ -k_s S[X2] + D_{X2}\frac{\partial^2[X2]}{\partial\theta^2} &= 0, \quad (L-L_1)/2 \le \theta < L/2 \end{aligned} \tag{14}$$

The first equation has been written, eliminating $[X1]$. This is supplemented by no-flux boundary conditions at the two ends (for simplicity the problem is analytically solved in half the domain, applying no flux boundary conditions).

The solution to these equations can be obtained by solving them in a piece-wise manner and matching them at the two interfaces. Thus the solution is obtained as

$$\begin{aligned} &[X2] = -(k_o/2D_{X2})\theta^2 + C_1\theta + C_2, \quad 0 \le \theta < L_1/2 \\ &[X2] = c_3\theta + c_4, \quad L_1/2 \le \theta < (L-L_1)/2 \\ &[X2] = c_5 exp(-\sqrt{(}k_s S/D_{X2})x) + c_6 exp(\sqrt{(}k_s S/D_{X2})x, \quad (L-L_1)/2 \le \theta < L/2 \end{aligned} \tag{15}$$

The net steady state solution can be obtained by matching the concentration and flux at the two interfaces. We will not present the detailed expression here, as the main observations can be obtained from the

expression above. We note that the overall profile (in each of the locations) depends on all the parameters in the above equation (through the matching conditions).

We see here that $[X3]$ can be easily obtained from the $[X2]$ concentration in the last subdomain, and is in fact proportional to it, with a proportionality factor depending on S. The point to note is (i) The solution is dependent on the absolute value of S and (ii) The solution also depends on the absolute value of the diffusion coefficient. We can therefore say that even though the average concentration of X3 exhibits an adaptive response, the local concentration of X3 at any specified location in the second location does not, in fact, adapt. In fact many characteristics of $[X3]$, such as the slope of the profile, do depend on S. Secondly, if the diffusion coefficient of X2 is very high, then the profile of X2 equilibrates at a level equal to $k_o/(k_s[S])$. This can be seen from the original equation in the limit of high D_{X2} by using a perturbation expansion in $1/D_{X2}$. In this case the steady state profile of $X3$ is spatially uniform at a level k_o/k_d. We therefore see how spatial separation can distort the local adaptive response, and how a high diffusion of communicating species can make the response close to adaptive.

In general we find that step changes in S result in overadaptive responses for $[X3]$ in some parts of the second domain (for instance in the middle, as shown in Fig. S4) and in underadaptive responses in others.

Now if we examine an analogous situation to the one above, but where the signal mediates the modification from $X1$ to $X2$, we find that $[X2]$ attains a profile independent of the signal, irrespective of the diffusion coefficient. Therefore, we find that $[X3]$ actually adapts to a step change in S, even though it does not have a uniform profile in the second compartment. This is seen by noting that the steady state profile of the diffusing species is independent of S. This is seen immediately by inspecting the equations for $[X2]$ in this case:

$$\begin{aligned} k_o + D_{X2}\frac{\partial^2[X2]}{\partial\theta^2} &= 0, \quad 0 \le \theta < L_1/2 \\ D_{X2}\frac{\partial^2[X2]}{\partial\theta^2} &= 0, \quad L_1/2 \le \theta < (L-L_1)/2 \\ -k_2[X2] + D_{X2}\frac{\partial^2[X2]}{\partial\theta^2} &= 0, \quad (L-L_1)/2 \le \theta < L/2 \end{aligned} \tag{16}$$

Note that $[X1]$ has been eliminated in the first equation. We see that this equation is independent of S and hence so is $X2$, even though the profile is not homogeneous. Therefore step changes in S result in locally adaptive responses for $X3$.

Overall, we see how, depending on the position of the signal in an open spatial cascade, one can maintain adaptive responses in some cases, and distort it in others. In contrast, exact adaptive responses result when the entire cascade is spatially localized in one location, irrespective of the position of the signal in the cascade. The diffusivity of $X2$ can affect the amplitude of the transient response of $X3$. If the diffusivity is lowered, the amplitude is lowered. This is because a low diffusivity means that a change in signal causes a practically exact adaptive response of $X2$ in location 1 (its dynamics there essentially governed by the kinetics), and any weak residual effect is slowly communicated to $X3$ through diffusion. Numerical results for the open irreversible cascade are shown in Fig. S4.

2.4 Communicating layer of cascade with multiple diffusing entities

While examining spatially separated model of cascades, we examined situations where the output of one level of the cascade acted as the communicating species. We now examine a variant of this scenario where both the modified and unmodified form are diffusible. In this case the two segments of the cascade may be regarded as being connected via a global layer.

We therefore examine the dynamics of this global layer. For simplicity we will assume that all relevant reactions involving the interconversion of these species act via mass action kinetics, and there is negligible retroactivity in the downstream reaction. We will refer to the species as X and X^* and assume both have the same diffusion coefficient D. At steady state we have

$$\begin{aligned} -k_f K(\theta)[X] + k_r P(\theta)[X^*] + D\frac{\partial^2[X]}{\partial\theta^2} &= 0, \\ k_f K(\theta)[X] - k_r P(\theta)[X^*] + D\frac{\partial^2[X^*]}{\partial\theta^2} &= 0 \end{aligned} \tag{17}$$

Here $K(\theta), P(\theta)$ refer to the kinase and phosphatase profiles. When we consider cascades of the kind examined earlier, $K(\theta)$ will be non-zero only in the first location.

By adding the above equations we find that at steady state $X + X^*$ is a constant, uniform in space. We call this constant X_T. Therefore the equation simplifies to

$$k_f K(\theta)(X_T - [X^*]) - k_r P(\theta)[X^*] + D\frac{\partial^2[X^*]}{\partial\theta^2} = 0 \tag{18}$$

We will focus on some specific aspects of the profile of X^*. In general, in such a scenario, we may expect different possibilities for where the phosphatase is located. It may be located everywhere in the

domain, it may be located in the second location, or it may be located in the first location.

In the case where the phosphatase is present everywhere in the domain, the above steady state can be obtained, and the resulting profile depends on the diffusion coefficient (see Fig. S5). Similarly when the phosphatase is in the second location only, the profile obtained, depends on all parameters, and depends on the diffusion coefficient. In both cases, when the diffusion coefficient becomes high, X^* attains a profile which is uniform.

In the case where the phosphatase is co-localized with the kinase, in the first location, we notice something different. When the kinase and phosphatase profile is uniform in this location, we have

$$[X^*] \quad = \quad X_T \frac{K/P}{k_r/k_f + K/P} \tag{19}$$

The point to note is that this concentration profile is uniform in space, and this is independent of the diffusion coefficient value. Thus we find that co-localizing the kinase and phosphatase of a global communicating layer can insulate the cascade from the effects of diffusivity at steady state. This points to another aspect of design and spatial organization of cascades. We mention one further point in this regard. If we compare this cascade, with a completely co-localized cascade, with the same total amount of X species in the medium (and of course all other factors the same), we find that the spatially distributed cascade involves a dilution effect. This is because the factor X_T is reduced (relative to the co-localized case) due to the fact that the X species is present in the entire medium.

2.5 Response of a modification cascade to spatial gradients

As mentioned in the paper, our framework allows us to also examine aspects of spatial signal transduction in cascades, without localization. We consider one such aspect here.

Diffusion and retroactivity in cascades. Although most of our focus in the paper is on effects of localization, there are other aspects to spatial signal transduction in cascades. One aspect which we briefly discuss is the response of a two tier cascade to spatial gradients. In this case all species are present everywhere in the spatial domain (i.e. no localization). Thus, we consider the same model of the cascade, with all components present everywhere in the domain. The input is provided in the form of a spatial gradient. When none of the signalling components diffuse, then the signal transduction is purely local, and can be studied using ODEs. On the other hand, as we have shown previously (1), diffusion of individual components can significantly alter and distort signal transduction. When we examine signal transduction in

such a cascade, the effects of diffusion of multiple components can be studied, some which can be simply understood from an equivalent study of a single covalent modification cycle (undertaken in (1) and others which rely on the interplay of the two cycles. We discuss one example of the latter.

The effects of diffusion perturbing the first modification cycle can largely be understood by the consideration of a single covalent modification cycle. When we examine the effects of diffusion of species in the downstream covalent modification cycle, some subtle features arise. When the species in the second step Y and X^*Y (the unmodified substrate at the second tier and the relevant complex) diffuse while all other species are weakly diffusible, (Figure S6), we find that the spatial profile of Y^* weakens. Further, the profiles of the species in the upstream cycle change- X becomes sharper, X^* becomes flatter and profiles of complexes in the first cycle are also affected. The underlying reason for the change in profiles of species upstream is that X^* is sequestered in the complex X^*Y. Thus in this case diffusion affects the profile of X^* having a ripple effect on the remaining species in the first step.

This demonstrates how diffusion of species in a signalling cascade can significantly affect species upstream and illustrates one example of the spatial dimension to retroactivity. While the effect of retroactivity has been much studied in kinetic terms, this example shows how diffusion of species in a cascade can have backpropagating effects. In the above example the reference case chosen was one where all other species were weakly diffusible, but the broader conclusion of the back propagating effects of species diffusion remains valid in other scenarios as well. This highlights one aspect of the effect of diffusion in signalling cascades.

2.6 Multisite modification with localization of kinase and phosphatase

The primary focus in the paper has been on the effects of localization in cascades and pathways. When we considered multisite modification, we examined the case where different enzyme pairs were localized in different locations. Here we briefly discuss the situation where there is double site modification by a common enzyme pair, with the kinase and phosphatase localized in different locations. The case of a single site modification with localized kinase and phosphatase in different locations has already been studied in (1).

We briefly consider a two site ordered mechanism of multisite modification by the same kinase and phosphatase pair (See Supplementary Figure S7). We examine two cases. If the kinase is colocalized with the unmodified substrate and the doubly modified substrate is the only substrate species diffusing, then it diffuses to the location of the phosphatase and is completely converted back to the unmodified substrate. If

both unmodified and doubly modified substrates diffuse (and the singly modified substrate does not), then the cycle can be completed. This is an example of spatial localization in multisite phosphorylation different from the ones considered above and is a simple multisite analogue of spatially separated kinase phosphatase pairs in covalent modification cycles seen in bacteria. We find here, that even though the cycle is complete, the behaviour is not a simple analogue of that situation. In fact we observe that singly modified substrate accumulates along with the kinase as well as phosphatase and both modified and double modified substrates exhibit weakly graded profiles. This feature is broadly seen in various parameter ranges, and simply relies on the fact that the partial phosphoform, being non-diffusible, is present at the sites of production, which correspond to the presence of kinase (which produces this phosphoform from unphosphorylated substrate and further modifies it) or phosphatase (which produces this from maximally phosphorylated substrate, and further dephosphorylates it). This can be seen transparently analytically when the various reactions occur via mass-action kinetics, but of course does not rely on this assumption. If all modified and unmodified substrates diffuse, then this is no longer the case. This points to another facet of the interplay between spatial control, localization and chemical modification sequences.

3 Parameter Values

Parameters and Additional Information about the Models:

In this section details about parameter values used in individual figures are presented. All equations are non-dimensionalized, and the appropriate parameter values are dimensionless. Most of the essential trends seen here are seen for other parameter values (diffusion coefficients, kinetic parameters, where applicable). This has been demonstrated analytically. The various parameters are presented in the Models section. Fig S1 depicts a subset of these models with parameters

Two Step Cascade (Figure 2):

$k_1 = k_3 = k_5 = k_7 = 0.1, k_{-1} = k_{-3} = k_{-5} = k_{-7} = 1.0, k_2 = k_6 = 0.05, k_4 = k_8 = 0.1$; Total Substrate = 2.0; Total Kinase= 1.0, Total Phosphatase P1=0.3, Total Phosphatase P2=0.5. A range of diffusion coefficients were tested from low $D_{X*} = 0.01.$ to intermediate $= 0.1, 1.0$ to high 10.0 for all figures. A: width of localized patches is 1/5th of domain length.

Three Step Cascade (Figure 3): The three step enzymatic cascade is an extension of the earlier studied two-step enzymatic cascade with an additional third stage (equations not shown). The parameter denominations for the first two stages are the same as in the two step cascade. In the third stage, the

substrate species are Z, Z^*, ZY^* and Z^*P3 and P3 is the phosphatase of the last step. The association rate constants (for phosphorylation/dephosphorylation) are k_9 and k_{11}, the dissociation rate constants are k_{-9} and k_{-11}, and the catalytic constants are k_{10} and k_{12}. The diffusion coefficients of the species in the last stage are $D_Z, D_{Y*Z}, D_{Z*}, D_{P3}$ and D_{Z*P3}. Parameter values are based on Huang and Ferrell. The association rate constants for step 1 (X and X^*) of the cascade are: $k_1 = k_3 = 1000$; for step 2 (Y to Y^*) are $k_5 = k_7 = 1000$; and for step 3 (Z to Z^*) are $k_9 = k_{11} = 1000$. The dissociation rate constants for each step are $k_{-1} = k_{-3} = 150$ (step 1); $k_{-5} = k_{-7} = 150$ (step 2) and $k_{-9} = k_{-11} = 150$ (step 3), and the catalytic constants are (step 1) $k_2 = k_4 = 150$; (step 2) $k_6 = k_8 = 150$ and (step 3) $k_{10} = k_{12} = 150$. Total Substrates $X^* = 0.003, Y^* = Z^* = 1.2$, Total Phosphatases $P1 = P2 = 0.0003, P3 = 0.12$. A: width of localized patches is 1/5 th of of domain length. B: width of patches is 1/50th of domain length.

Three Step Cascade with a transient input (Figure 3C and D): For this analysis, the first reaction in the first step (X is converted to X*) in the three step cascade model is modified. For simplicity, the reaction is in the mass action regime. This allowed us to directly regulate the free/total Kinase concentration [K] (which is the transient input). $[K] = 0.0001$, forward rate constant associated with K, $k_1 = 1000$. Spatial design III was studied and a pulse duration of t=10 was applied. In Fig. 3C, the diffusivity of X^* was varied and in Fig. 3D the spatial width of the patch was varied (as a fraction of domain length) . The rest of the parameters are same as in Figure 3

Multisite phosphorylation (Figure 4):

(A,B): $k_1 = k_3 = k_5 = k_7 = 0.1, k_{-1} = k_{-3} = k_{-5} = k_{-7} = 1.0, k_2 = k_6 = 0.05, k_4 = k_8 = 0.1$; Total Substrate = 2.0; Total Kinase K1= 1.0, Total Phosphatase P1=0.3, Total Kinase K2= 1.0; Total Phosphatase P2=0.5.

C: $k_1 = k_3 = k_7 = 1.0 k_5 = 0.2, k_{-1} = k_{-3} = k_{-5} = k_{-7} = 1.0, k_2 = k_6 = 0.05, k_4 = k_8 = 0.1$; Total Substrate = 2.0; Total Kinase K1= 0.5, Total Phosphatase P=0.3, Total Kinase K2= 0.5; C: width of localized patches is 1/5th of domain length. Diffusion coefficient of diffusing species is 0.01.

Phosphorelay (Figure 5):

4-step relay (Fig. 5 C): $k_s = 1.0 = k_1 = k_3 = k_5 = k_{p1} = k_{p3} = k_{p5} = k_{p7} = 0.1$, the dissociation rate constants are $k_{-1} = k_{-3} = k_{-5} = k_{-p1} = k_{-p3} = k_{-p5} = k_{-p7} = 1.0$ and the catalytic rate constants are $k_2 = k_4 = k_6 = 0.05, k_{p2} = k_{p4} = k_{p6} = k_{p8} = 0.1$. Total Substrates $X1 = X2 = X3 = X4 = 2.0$; Input signal $K = 1.0$, Total Phosphatase $P1 = P3 = P4 = 0.3$, Total Phosphatases $P2 = 0.5$.

In a 2 step relay (Fig. 5 A,B) the parameters associated with steps 3 and 4 are zero and the remaining parameters are the same as Fig. 5C: Thus $k_3, k_5, k_{p5}, k_{p7}, k_{-3}, k_{-5}, k_{-p5}, k_{-p7}, k_4, k_6, k_{p6}, k_{p8}$. are all 0.

A, B and C: width of localized patches is 3/10th of domain length.

Supplementary Figures

Figure S2: $k_1 = k_3 = 10.0, k_{-1} = k_{-3} = 1.0, k_2 = k_4 = 0.1$ Total Substrate $= 2.0$, Total Phosphatase $P = 0.03$. Width of the localized patch is 1/5th of domain length. A range of diffusion coefficients were tested from low $D_{X*} = 0.01$ to intermediate $= 0.1 and 1.0$ to high 10.0. The diffusion coefficient shown here is D$= 1.0$.

Fig. S3. The kinetic parameters used are those in Fig. 3 C, D. In (b) the duration of the pulse is varied.

Figure S4: Top row: $k_o = 0.1; S = 0.2; k_s = 1.0; k_2 = 0.5, k_d = 1.0$. Row 2: $k_o = 0.1; S = 0.2; k_1 = 0.5; k_s = 1.0; k_d = 1.0$. RHS plots: $D_{X2} = 0.01$ (solid line) and $D_{X2} = 10.0$ (dashed line) Width of localized patches is 1/5th of domain length. The basal level of the signal was $S = 0.1$.

Figure S5: (A and B) $k_1 = k_3 = k_7 = k_{11} = 0.1, k_5 = 0.2$ and $k_9 = 0.3$, the dissociation rate constants are $k_{-1} = k_{-3} = k_{-5} = k_{-7} = k_{-9} = k_{-11} = 1.0$, and the catalytic constants are $k_2 = k_6 = k_{10} = 0.05, k_4 = k_8 = k_{12} = 0.1$. Total Substrates $X^* = 2.0, Y^* = 1.0; Z^* = 1.2$, Total Phosphatases $P1 = 0.5; P2 = 1.0, P3 = 0.5$, Total Kinase $K = 1.0$. The diffusion coefficients of Y and Y* are equal and are D=0.01 (solid line), D=0.1 (dashed line), D=1.0 (crosses) and D=10.0 (solid line with circles). Width of localized patches is 1/5th of domain length.

Figure S6:

$k_1 = k_3 = k_7 = 0.1, k_5 = 0.2, k_{-1} = k_{-3} = k_{-5} = k_{-7} = 1.0, k_2 = k_6 = 0.05, k_4 = k_8 = 0.1$; Total Substrate $X = 2.0$; Total Kinase $K = 1.0 + 0.3 cos\theta$, Total Substrate $Y = 1.0$; Total Phosphatase $P1 = P2 = 1 + 0.2Cos(\pi + \theta)$. All upstream X species are weakly diffusing at $D_{X*} = 0.001$ and Y and YX* diffuse at $D = 1.0$.

Figure S7:

$k_1 = k_3 = k_7 = 0.1, k_5 = 0.2, k_{-1} = k_{-3} = k_{-5} = k_{-7} = 1.0, k_2 = k_6 = 0.05, k_4 = k_8 = 0.1$; Total Substrate $= 2.0$; Total Kinase K$= 0.5$, Total Phosphatase P$= 0.5$. The width of localized patches is 1/5 th of domain length. A range of diffusion coefficients were tested from low $D_{X*} = 0.01$ to intermediate $= 0.1 and 1.0$ to high 10.0. The diffusion coefficient shown here is D$= 0.01$.

Figure Legends

Figure S1

The depiction of the basic kinetic steps involved in (A) enzymatic cascades (B) multiple modifications of the substrate and (C) phosphorelays. Also depicted is that fact that these modifications may happen in two different compartments. The communicating species in each case diffuses from one compartment to the other,connecting the two stages of the cascade. Hence, it is present in both compartments.

Figure S2

A 2-step modification cascade where the first step is in the ultrasensitive regime, and the second step occurs via mass action kinetics is considered. We focus on the first step. The steady state input/output curve of [X^*] is shown. When none of the species diffuse (solid line), the module shows an ultrasensitive response. If X^* itself diffuses (solid line with triangle markers) the sensitivity of the input-output curve is greatly reduced. Therefore if X^* is the communicating species in a spatially separated cascade, the switch-like effect is severely attenuated.

Figure S3

Transient behaviour in 3 step cascades. (a) The effect of the patch width on the transient behaviour in spatial design IV is presented showing non-monotonic behaviour, similar to the case seen in the text. (b) The effect of variation of pulse duration shown for design II: as pulse duration increases the output acquires a clear plateau.

Figure S4

Open cascade. The transient behaviour of X3 is shown in response to a step change in signal. The first row shows the case where the signal S enters the cascade between X1 and X2 and the second row shows the case where S enters the cascade between X2 and X3. The column on the left shows the case when all the species are localized together; X3 shows an adaptive response. The plots in the right column show the case where X1 and X3 are in two different compartments. [X3] in the middle of the second domain is shown. (Top RHS plot) X3 does exhibit an adaptive response and its amplitude is higher for higher diffusivities of X2 (dashed line) and low when X2 diffusion is weak (solid line). In contrast, in the second case, for low

diffusion coefficients (solid line) X3 does not perfectly adapt while it essentially does for high diffusion coefficients (dashed line).

Figure S5

A three step cascade with a global second step, i.e. Y and Y^* both diffuse: the spatial concentration profiles of Y^* (second step) and Z^* (last step) are shown for different scenarios. (A) P2 is uniform and present everywhere in the domain. In the bottom LHS plot Z^* is in location 1 and in the bottom RHS plot Z^* is in the opposite location. The profile of the Z^* is determined by the diffusion coefficient values of Y and Y^* and its own position in the domain. The arrow denotes the direction of increasing diffusion coefficient for Y and Y^*. (B) P2 is in the second location and the resultant profile of Y^* is shown. The spatial profile of Z^* behaves in a similar fashion as in (A). Increasing the diffusion coefficient flattens the profile of Y^*. In these plots the $D = 1$ and $D = 10$ curves are practically indistinguishable.

Figure S6

Two step covalent modification cascade subject to a gradient: The enzymes are graded and of the form a+bCos(θ). The case depicted here is for when the phosphatase enzymes are counter-aligned with the input kinase profile. Spatial concentration profiles of species are shown for two cases- 1) All the species weakly diffuse (solid line) and 2) Y and YX^* both diffuse strongly (dashed line) (other species are weakly diffusing). In the latter case, the spatial concentration profiles of all species, including the species in the upstream step are modified. The spatial profile of X becomes enhanced and that of X^* becomes weaker. The spatial profile of Y^* becomes weaker as well. The effect of diffusion propagates upstream causing a modification of spatial profiles both upstream and downstream.

Figure S7

Double site modification with a single enzyme pair that are localized in opposite patches in the domain (K is localized on the left in the domain and P is on the right). All substrate is initially localized alongside the kinase.The spatial concentration profiles of species X, X^* and X^{**} are shown. When there is no diffusion (solid line), X^{**} profile is present where K is localized, X and X^* are zero at steady state. If both X and X^{**} diffuse (line with dots) then both spatial profiles are spread in the domain and X^* is localized in both locations.

References

1. Alam-Nazki, A., J. Krishnan, 2013. Covalent Modification Cycles through the Spatial Prism. *Biophys. J.*, 105:1720-1731.

Figure S1

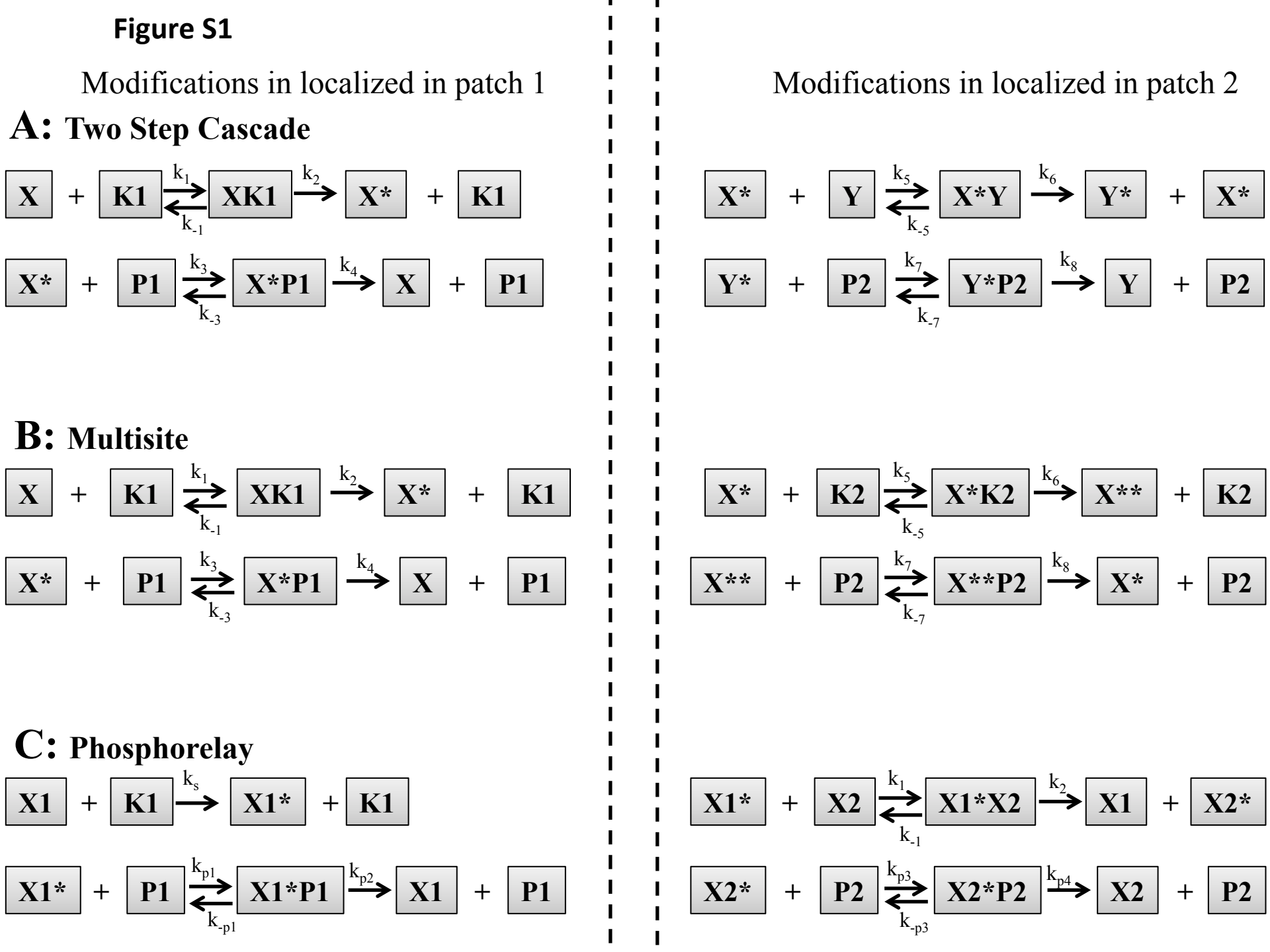
Modifications in localized in patch 1
Modifications in localized in patch 2
A: Two Step Cascade
X + K1 ⇄ XK1 → X* + K1
X* + P1 ⇄ X*P1 → X + P1
X* + Y ⇄ X*Y → Y* + X*
Y* + P2 ⇄ Y*P2 → Y + P2
B: Multisite
X + K1 ⇄ XK1 → X* + K1
X* + P1 ⇄ X*P1 → X + P1
X* + K2 ⇄ X*K2 → X** + K2
X** + P2 ⇄ X**P2 → X* + P2
C: Phosphorelay
X1 + K1 → X1* + K1
X1* + P1 ⇄ X1*P1 → X1 + P1
X1* + X2 ⇄ X1*X2 → X1 + X2*
X2* + P2 ⇄ X2*P2 → X2 + P2

Figure S2

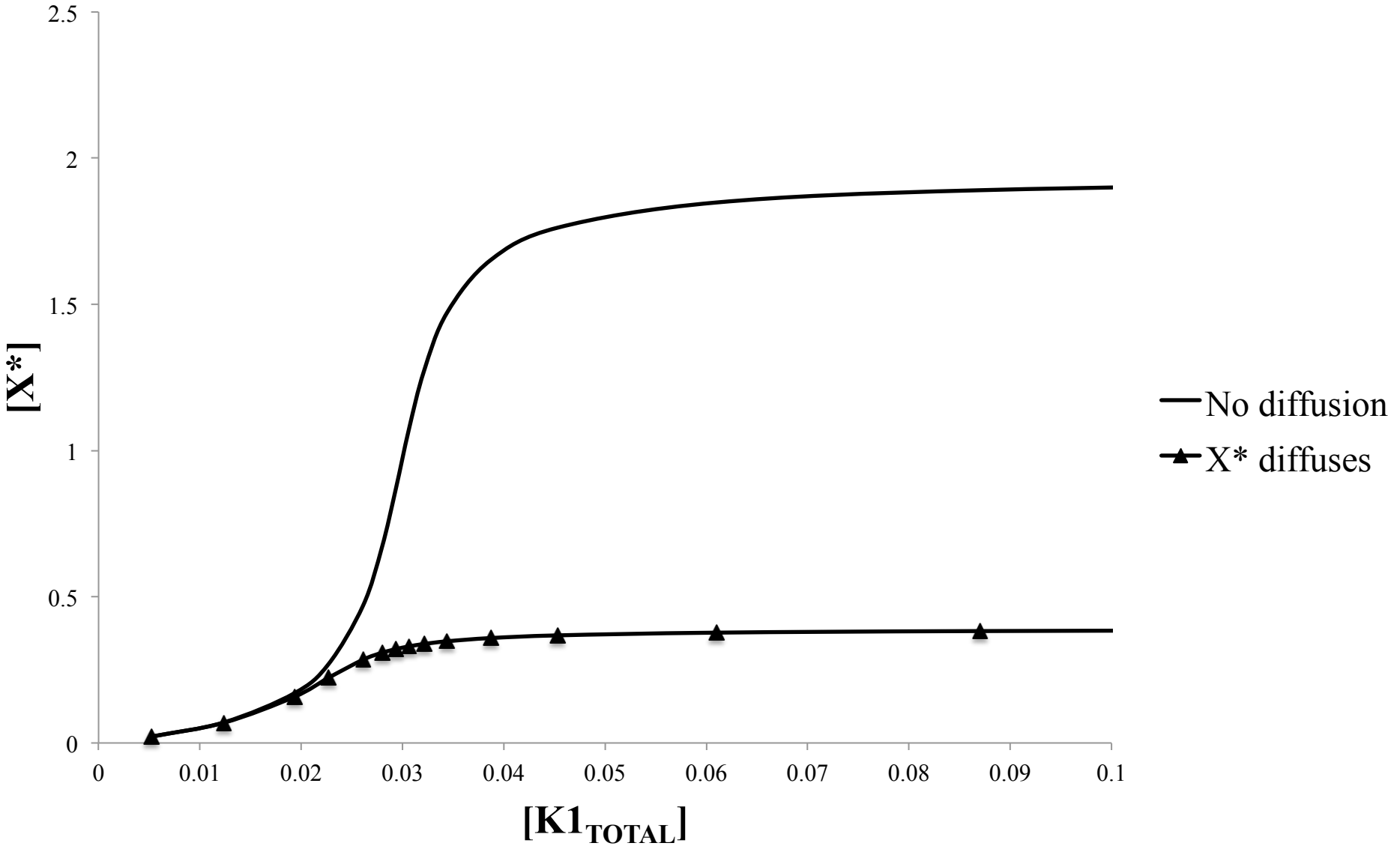
2.5
2
1.5
1
0.5
0
[X*]
0
0.01
0.02
0.03
0.04
0.05
0.06
0.07
0.08
0.09
0.1
[K1TOTAL]
No diffusion
X* diffuses

Figure S3

A

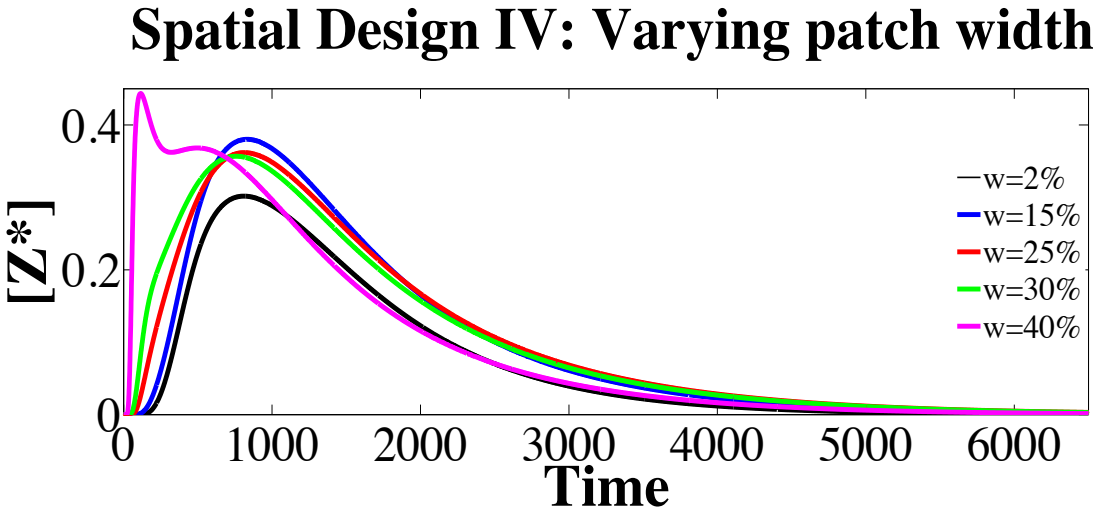
Spatial Design IV: Varying patch width
[Z*]
0.4
0.2
0
0
1000
2000
3000
4000
5000
6000
Time
w=2%
w=15%
w=25%
w=30%
w=40%

B

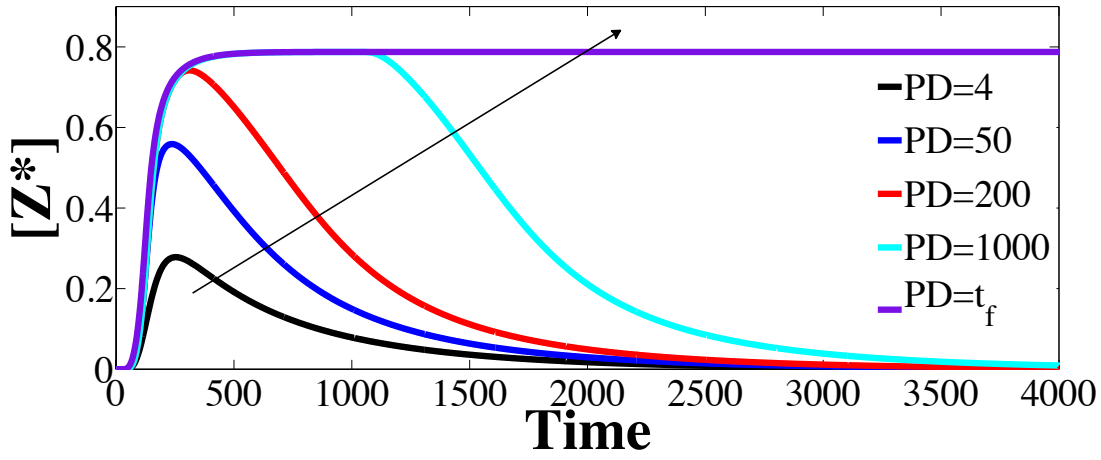
Spatial Design II: Varying pulse duration
[Z*]
0.8
0.6
0.4
0.2
0
0
500
1000
1500
2000
2500
3000
3500
4000
Time
PD=4
PD=50
PD=200
PD=1000
PD=t_f

Figure S4

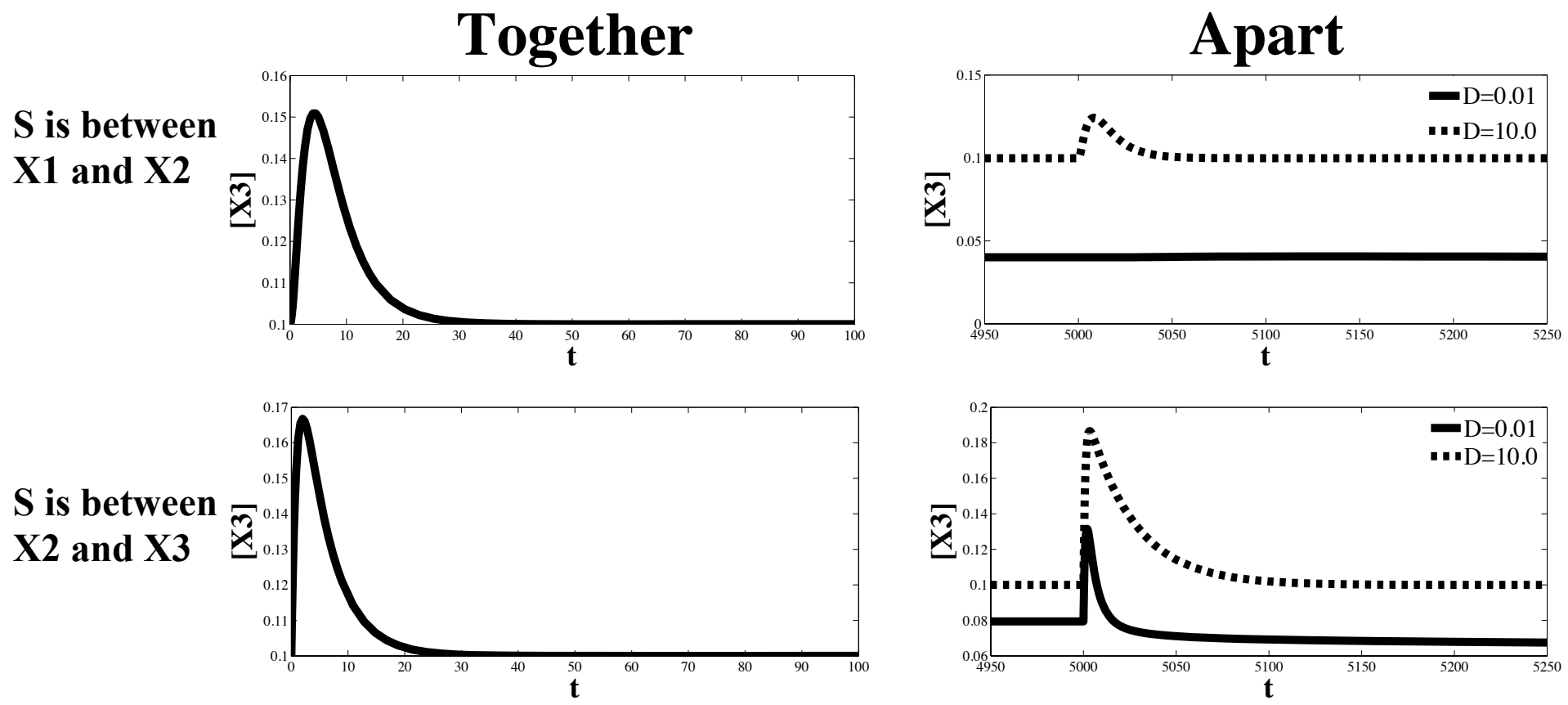
Together
Apart
S is between X1 and X2
S is between X2 and X3
[X3]
t
D=0.01
D=10.0

Figure S5

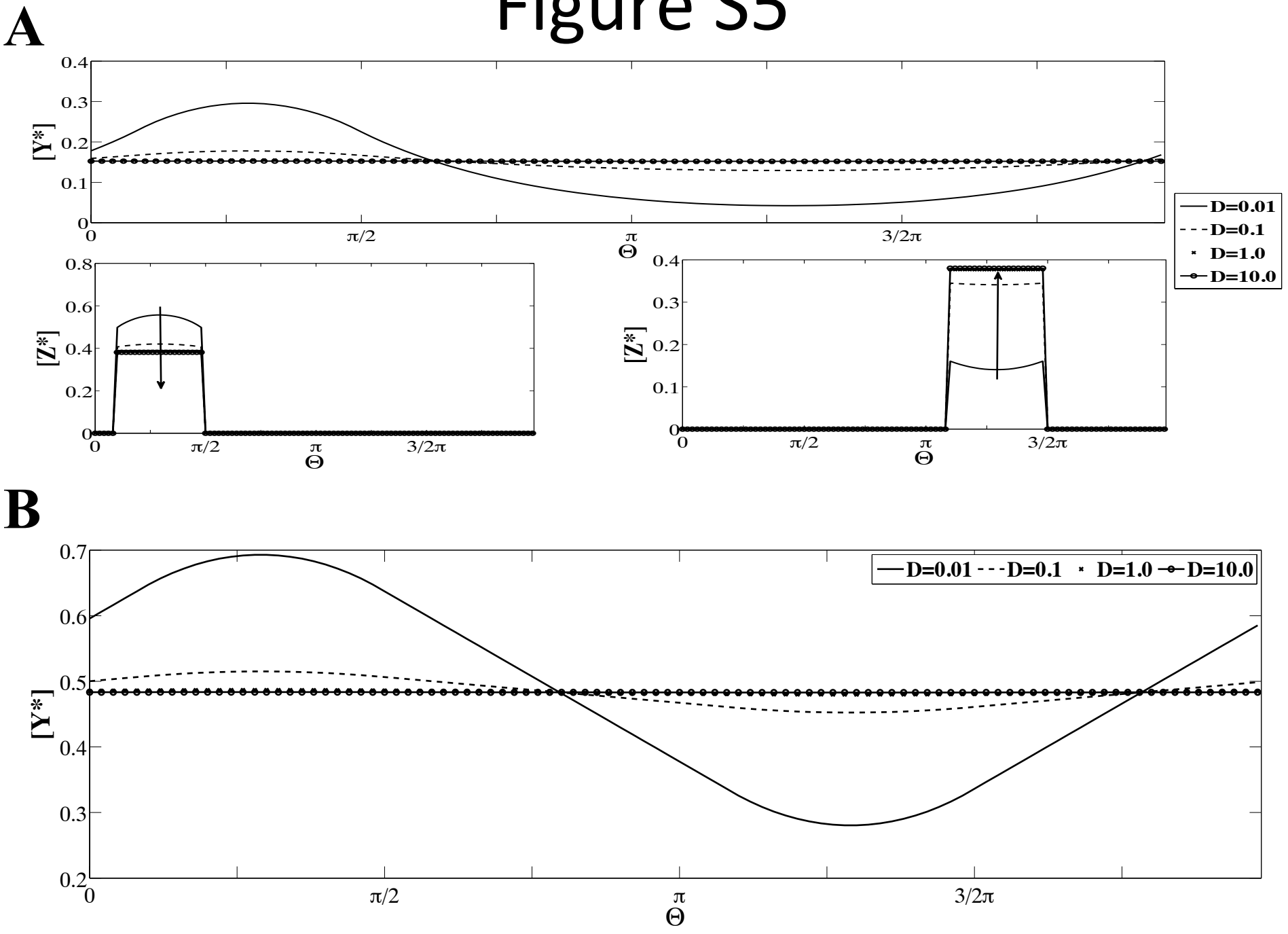

Figure S6

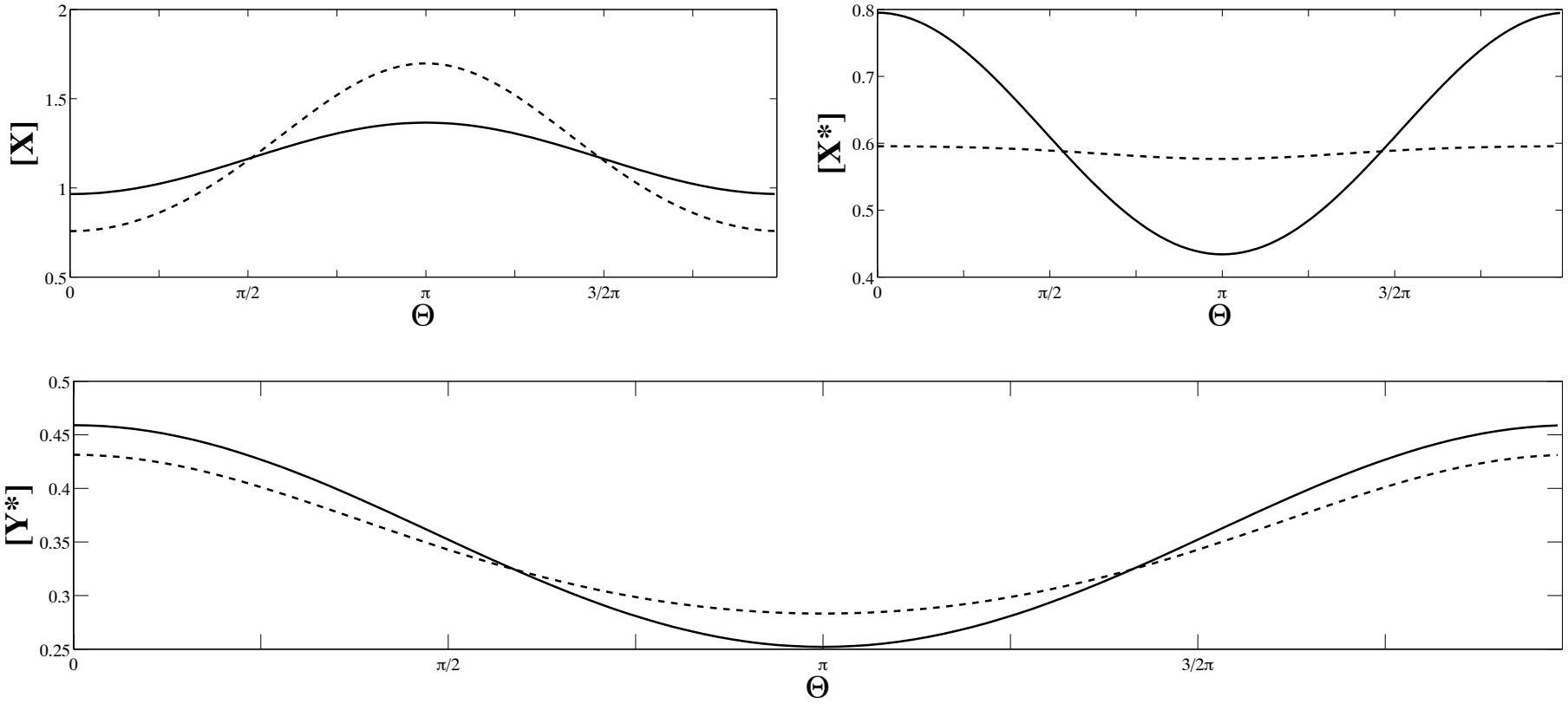
[X]
2
1.5
1
0.5
0
π/2
π
3/2π
Θ
[X*]
0.8
0.7
0.6
0.5
0.4
0
π/2
π
3/2π
Θ
[Y*]
0.5
0.45
0.4
0.35
0.3
0.25
0
π/2
π
3/2π
Θ

Figure S7

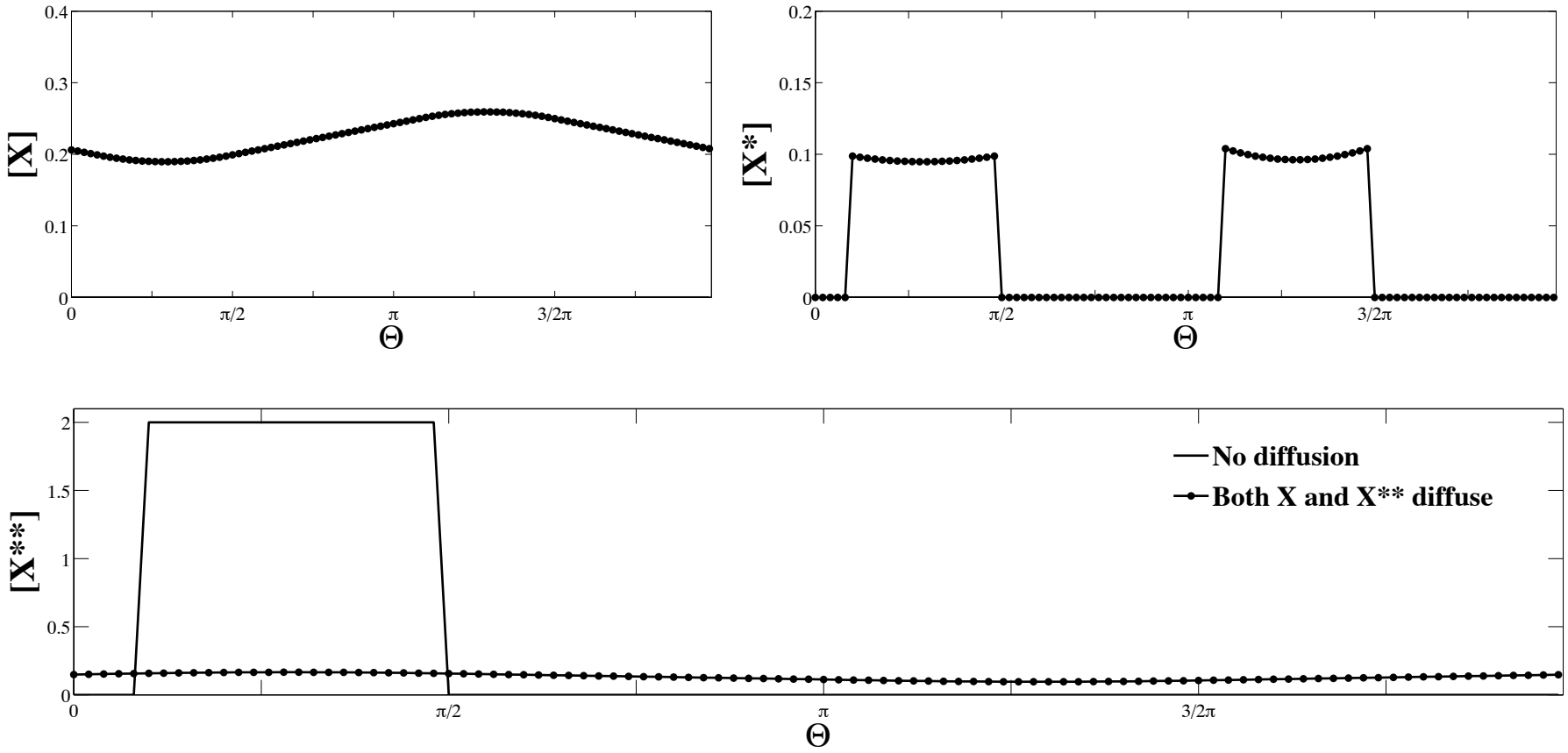
[X]
0.4
0.3
0.2
0.1
0
0
π/2
π
3/2π
Θ
[X*]
0.2
0.15
0.1
0.05
0
0
π/2
π
3/2π
Θ
[X**]
2
1.5
1
0.5
0
0
π/2
π
3/2π
Θ
No diffusion
Both X and X** diffuse

[P1]	Dx*=0 (Together)		Dx*=0.1 (Apart)	
	X*	Y*	X*	Y*
0.3	1.177	1.074	0.3461	0.5318
0.7	0.7548	0.8702	0.2996	0.478
1	0.5908	0.7578	0.2715	0.4434
1.5	0.4324	0.6214	0.2342	0.3948
2	0.3406	0.5256	0.2055	0.3551
3	0.2389	0.401	0.1645	0.2949
10	0.07719	0.15	0.06778	0.1329

Table S1: The effect of varying the concentration of P1 phosphatase on X* and Y* when the modifications are together and apart for a two-step cascade is shown. The effect of varying P1 concentrations in a two step spatial cascade is compared between the cases when both steps are localized in the same location (columns 2 and 3) and when they are separated (columns 4 and 5). Increasing P1 concentrations results in the steady state output of the separated cascade, becoming close to that of the completely localized cascade, both in absolute and relative terms.